University of Groningen

IEM Research Project

# Flexible bladder behaviour in shallow water conditions

*Author:*
Jaap Jonker

*First Supervisor:*
prof. dr. A. Vakis
*Second Supervisor:*
drs. W.A. Prins

March 30, 2021

rijksuniversiteit
groningen

**Abstract**

The Ocean Grazer battery is a novel design to store energy for supply at desired moments. The battery consists of three components which are a rigid reservoir buried beneath the seabed, a flexible bladder floating above the seabed and engine room which connects the two of them. The base principle entails that if the energy supply exceeds the energy demand, the abundant energy is used to pump a working fluid from the rigid reservoir to the flexible bladder. Due to the depth of the rigid reservoir, a pressure head arises which is used to let the working fluid flow back from the flexible bladder to the rigid reservoir at desired moments. During this back-flow the working fluid passes a turbine and energy is regenerated. This research focuses on the flexible bladder component of the battery.

Before the start of this research the Ocean Grazer research group proposed a preliminary design for the flexible bladder. The main problem is that for the preliminary flexible bladder design it is unclear how it can be completed to a suitable final bladder design. The bladder must be able to withstand all loads exerted from in- and outside the bladder, and to inflate/deflate in an optimal and durable manner. Therefore, in this research multiple design solutions are analysed and simulated in order to indicate which design solution has the most potential, taking into consideration the requirements set. The bladder design that eventually indicates the best performance, based on folding and deflation, is a bladder with end caps based on the shape of a toothpaste tube.

# Contents

# List of Figures

# List of Tables

# 1 Introduction

## 1.1 Sustainable Energy Consumption

Climate change is a widely discussed phenomenon in modern society. The effects of climate change become more evident over the years with significant loss of sea ice, accelerated sea level rise and longer, more intense heatwaves [1]. The impact by human kind on this climate change cannot be ignored due to the large consumption of fossil fuels. The enlargement of energy production that contains low carbon emission is an ongoing challenge, which in 2019 only results in one third of the electricity production. This number presumes that mankind is on the right track; however, a closer look at the total energy production indicates that more than 80% of the total energy production is still based on fossil fuels [2].
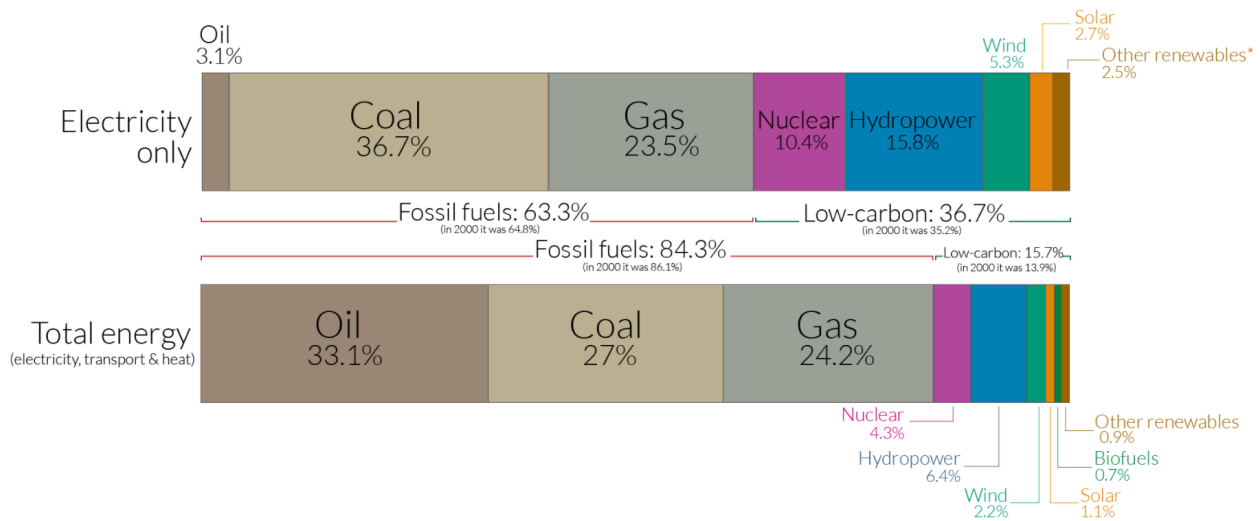


Figure 1: Worldwide energy consumption in 2019 [2].

In order to decrease the ratio between fossil fuels and low carbon fuels the development of sustainable energy production methods continues. Another aspect is the supply and demand of energy. The energy demand is not a constant value, energy demand fluctuates with a higher demand during the day and a lower demand overnight. Moreover, there is a clear seasonality in energy demand with a higher demand during the colder months [3]. The energy production on the other hand is not constant neither with changes in amount of wind and solar. The fluctuations in supply and demand lead to occasional surplus of energy, which is difficult to store for later usage. Therefore, the development of methods to store surplus energy is essential to cope with the problem of energy waste.

## 1.2  Ocean Grazer Battery

The Ocean Grazer (OG) battery is a novel design to store electric for supply at desired moments. The basic principle entails that if the energy supply exceeds the energy demand, the abundant energy is used to charge the battery. The battery consists of three components which are a rigid reservoir, an engine room and a flexible bladder. The abundant energy is used to drive a pump in the engine room that pumps a working fluid form the rigid reservoir to the flexible bladder. The rigid reservoir is buried under the seabed; however it communicates with the atmosphere by an umbilical cord. This results in a pressure head equal to the depth of the rigid reservoir. The pressure difference is used for back-flow of the working fluid from the flexible to the rigid reservoir. This back-flow can be activated at a desired moment whereby it passes a turbine, and therefore generates energy.

# 2  Research Design

In order to perform this research in a structured way, the Engineering Cycle is used as a clear road-map for the sequence of steps to take. The main reason that the Engineering Cycle has the best fit for this research is because there is no need for a diagnostic phase, as the problem is globally known from the beginning of the research: the preliminary design for the flexible bladder has not been examined taking into consideration the requirements set for shallow water conditions. The Engineering Cycle is a rational problem-solving process which provides a clear guidance for the research [4]. It consists of five phases where in the first phase the problem is thoroughly investigated. Subsequently, in treatment design the requirements are determined and the actions to develop the new design take place. During treatment validation it is checked if the new designs fulfill the goals and requirements set in the previous steps. After the validation a new design is implemented in a experimental situation where-after the evaluation phase determines if the desired effect is achieved. Due to Covid-19 regulations it is doubtful if the implementation phase will be reached. If it turns out that the development of a prototype is not realizable, this research ends at the treatment validation phase.

**Treatment implementation**

**Implementation evaluation / Problem investigation**
- Stakeholders? Goals?
- Conceptual problem framework?
- Phenomena? Causes, mechanisms, reasons?
- Effects? Contribution to Goals?

**Treatment validation**
- Artifact X Context produces Effects?
- Trade-offs for different artifacts?
- Sensitivity for different contexts?
- Effects satisfy Requirements?

**Treatment design**
- Specify requirements!
- Requirements contribute to Goals?
- Available treatments?
- Design new ones!

Figure 2: The Engineering Cycle [4].

# 3 Problem Investigation

## 3.1 Stakeholder Analysis

The stakeholder analysis is an important tool to identify all relevant stakeholders and the impact of their dynamics [5]. The first stakeholder is the CTO of OG BV: M. van Rooij. As a representative of the company Marijn benefits from all new knowledge that contributes to the development of the OG battery. A preliminary design for the flexible bladder takes the company one step closer to the realization of putting the OG battery into operation and getting revenue out of the concept.

The second stakeholder is drs. W.A. Prins. As founder of the original OG concept, drs. W.A. Prins is still fully involved in the project providing weekly advise and insights as scientific advisor on behalf of the OG BV. Furthermore, drs. W.A. Prins is the second supervisor of this research.

The third is prof. dr. A. Vakis, as first supervisor and part of the OG research group he is responsible for applying appropriate feedback on this research in order to help getting this research to the sufficient academic level. Furthermore, the knowledge gained in this research could be helpful for the OG research group as well.

The stakeholder power-interest grid in figure 3 is used to categorize the different stakeholders [5]. The upper two blocks have the most interest or so called stake in the organization and the blocks on the right hand have more power to affect the organizations strategy.
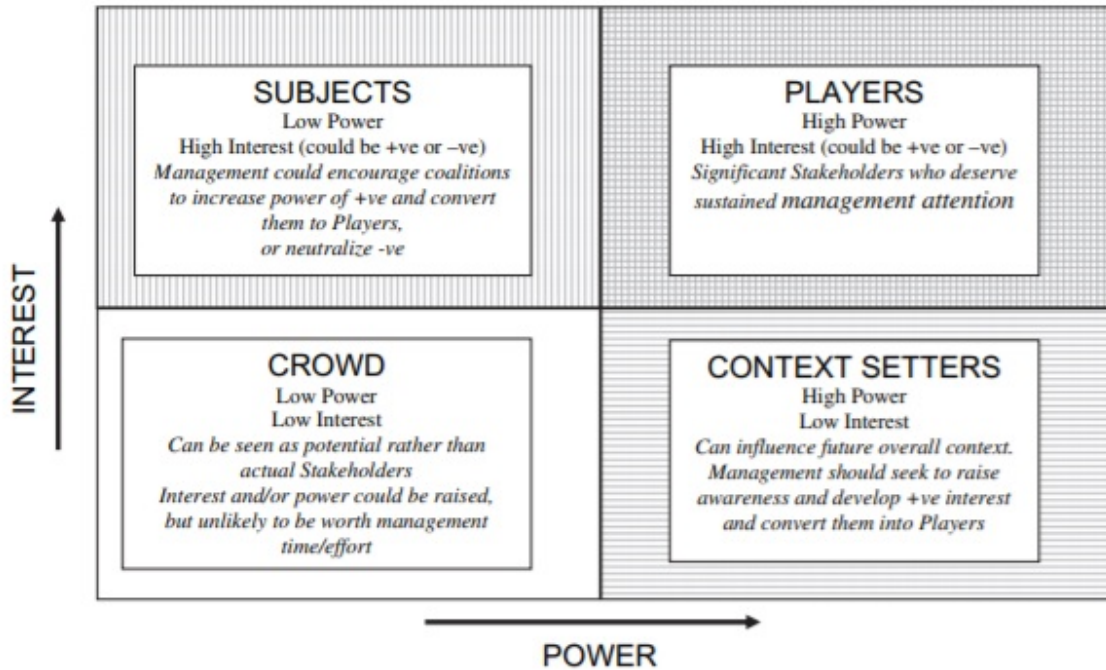
Figure 3: Stakeholder Power-Interest Grid [5].

According to figure 3 all three of the stakeholders can be considered as players. The supervisors are the persons grading this research. Therefore, the research has to be according to their standards which means they have 'high power'. On the other hand they have 'high interest' in this research since the outcome could be beneficial for the ongoing process within the OG research group.

CTO M. van Rooij and scientific advisor drs. W.A. Prins can also be categorized as players since they both provide knowledge and feedback from within the company and have a serious impact on the direction of this research, which can be labeled as 'high power'. In reverse, the outcome of this research can be a crucial part in the development of the OG Battery, which means they have 'high interest'.

## 3.2 System Description

### 3.2.1 General principle

Working fluid in a Rigid reservoir (1) buried beneath the seabed is pumped into a flexible bladder (2) that floats above the seabed. Between the rigid reservoir and the flexible bladder there is an engine room (3) that connects both sections. Pumps and turbines are located in the bottom of the engine room able to pump all the working fluid of the rigid reservoir into the flexible bladders. When the working fluid is in the flexible bladder it can be released to the rigid reservoir at a desired moment passing the turbines, and generating energy. The working fluid is driven from the flexible bladder to the rigid reservoir by means of a pressure difference that occurs due to fact that the rigid reservoir is

under atmospheric pressure by an umbilical cord. Furthermore, hydro-static pressure exerts a force on the outside of the flexible bladder as well.
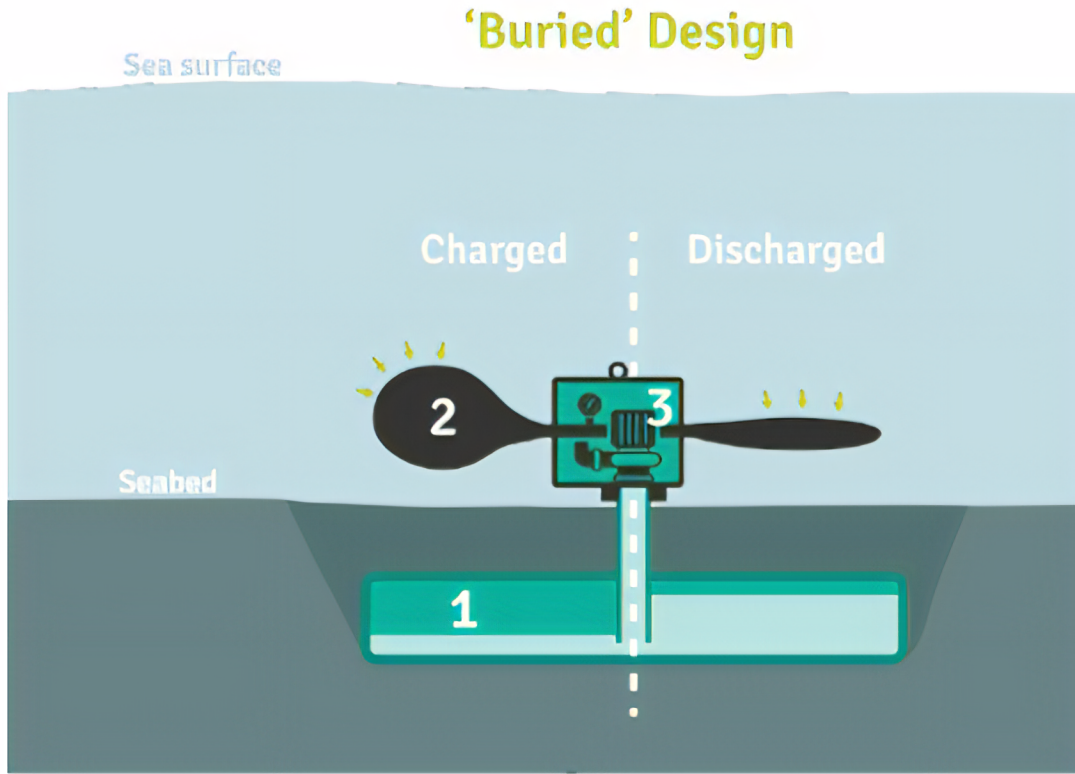


Figure 4: OG Battery.

### 3.2.2  Scope

The scope of this research will be solely on the flexible bladder. In figure 5 the situation for the flexible bladder is elaborated. Working fluid is pumped and stored in the flexible bladder were the working fluid exerts a force ($F_{WF}$) on the inside of the bladder. On the other hand there are multiple components applying force on the outside of the bladder. First of all, the gravitational force ($F_g$) acts on the bladder due to the mass of the whole structure. Second, the bladder tends to float due to the buoyancy force ($F_B$). Thirdly, the water column above the flexible bladder presses on the bladder by means of the hydro-static force ($F_H$). As fourth, the bladder is connected to the rigid reservoir with cables to keep it at the desired place. These cables function as anchor, and therefore apply an anchor force ($F_A$). Lastly, since the bladder is placed in the sea, forces of the current need to be taken into consideration. This force is indicated as current force ($F_C$).
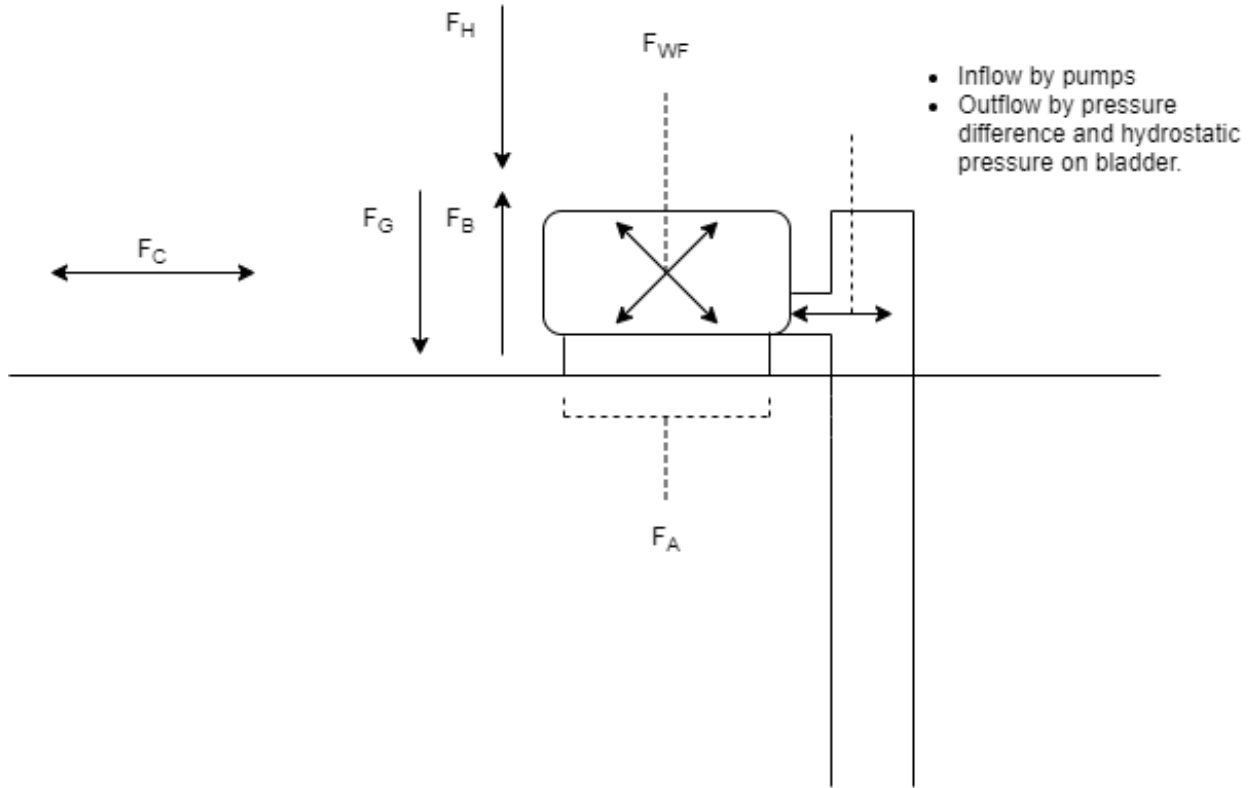
Figure 5: Scoped system.

### 3.2.3  Preliminary design

Before the start of this research the OG BV proposed a preliminary design that requires further development. The preliminary design consist out of bladder that is circular in inflated condition. In this circular design an air tube is fitted on top of the bladder and a drain tube is fitted in the bottom of the bladder. The drain tube is connected to the rigid reservoir with cables, which prevents the flexible bladder from drifting away from its desired position. On the other hand, the air tube has sufficient buoyancy force to keep the whole structure floating with respect to the seabed. When the bladder goes from the inflated state to the deflated stated the pressure of the working fluid on the inside of the bladder decreases, while the water pressure of the surrounding sea stays constant. This results in an inward movement of the bladder wall which could lead to folding. To prevent folding, the buoyancy force of the air tube must be large enough to stretch the wall vertically during the deflating process, such that a thin longitudinal shape occurs. During the inflation process the pressure of the working fluid on the inside of the wall causes the bladder to return to its original circular shape. A graphical representation of both states is depicted in figure 6.
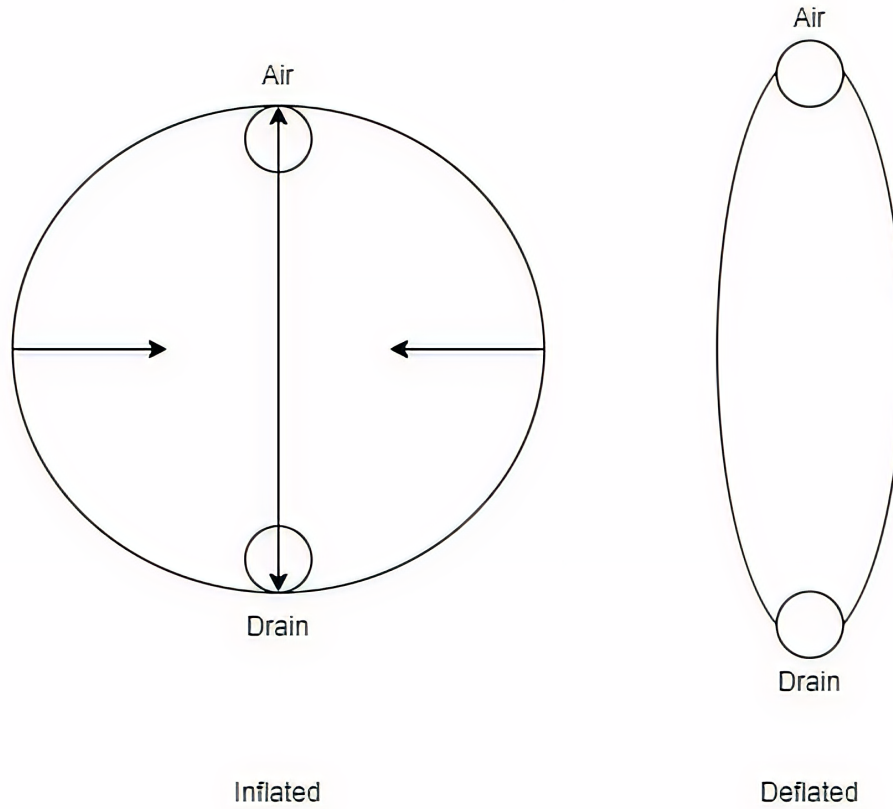
Figure 6: Preliminary design

## 3.3 Research Problem and Goal Statement

The main problem entails that with the current idea for the preliminary flexible bladder design it is unclear which final bladder design is best to withstand all forces exerted from inside and outside the bladder and is able to inflate/deflate in an optimal and durable manner. The DSR Knowledge Contribution Framework in figure 7 is used to classify the research regarding its theoretical contribution [6]. The x-axis shows the maturity of the problem context from high to low. The y-axis represents the current maturity of the artifacts that exist as potential starting points for solutions to the problem, also from high to low.
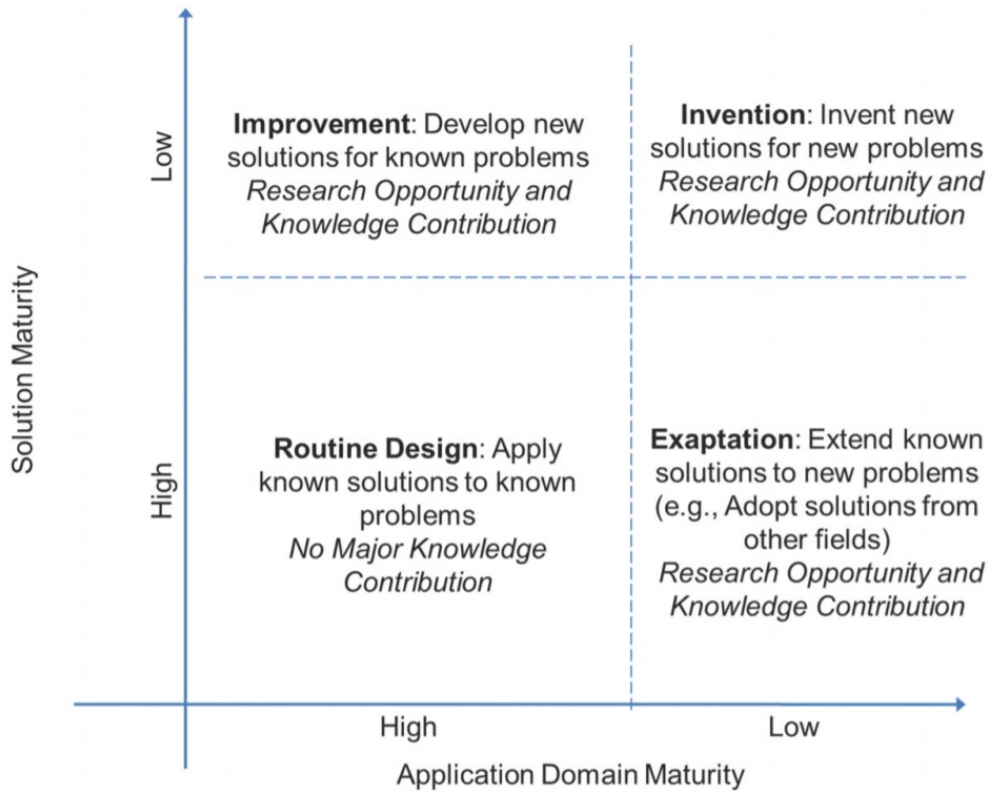
Figure 7: DSR Knowledge Contribution Framework [6].

The OG battery including the flexible bladder is a novel concept which has never been used in other application. While still in an early stage, it is basically pioneering to achieve a bladder that fulfills the goals. Therefore, on the x-axis there is low maturity. The solution to the problem is not developed yet either. Throughout literature there are a couple of suggestions concerning bladder shaped, nevertheless these solutions are applied in different circumstances and need further research to determine whether they are applicable to the flexible bladder of the OG battery. Therefore, on the y-axis there is low maturity. This leads to the result that the research fits in the category 'Invention' where new solutions are developed for new problems.

This leads to the following problem statement:
*The preliminary design for the flexible bladder has not been examined taking into consideration the requirements set for the shallow water conditions.*

To solve this problem, the goal of this research is defined as follows:
*To examine the design options that complement the preliminary flexible bladder design in order to deliver a design for further research.*

## 3.4  Research Question

The problem statement and goal can be translated to an overall research question that takes the complexity of the problem into consideration.

The research question is formulated as:
*Which design option is suitable to complement the preliminary design for the flexible bladder based on shallow water conditions?*

## 3.5  Knowledge Questions

To conduct the research in a structured way the research question is divided in three categories according to the Engineering Cycle; knowledge, design and evaluation questions. In the problem investigation phase the knowledge question will be discussed to collect all relevant information before proceeding to the treatment design phase. In this research the goal of the knowledge questions is to capture all the necessary information about the important aspects concerning size, shape, material and environment of the flexible bladder.

**KQ1**: Which bladder designs have been examined in previous OG research?

Over the years research on different types of flexible bladders have been examined within the OG research group. The research started with a circular design surrounding a rigid reservoir as depicted in figure 8. This first design indicated the potential of the idea; however, it also addresses the first problems that occurred during deflation due to bladder material blocking the outlet in the 90° corner of the support structure shown in figure 9 [7].
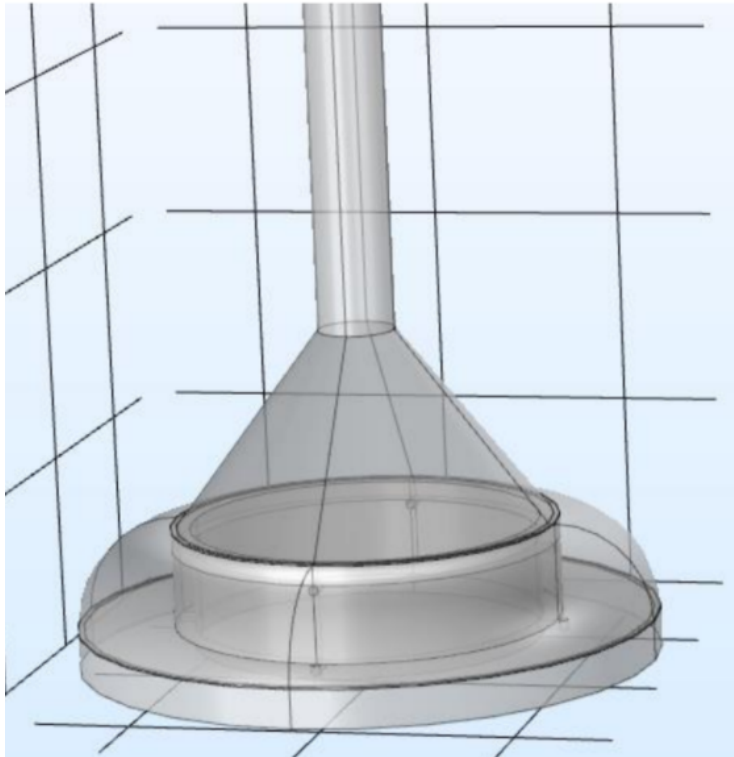
Figure 8: First circular design of the flexible bladder [7].
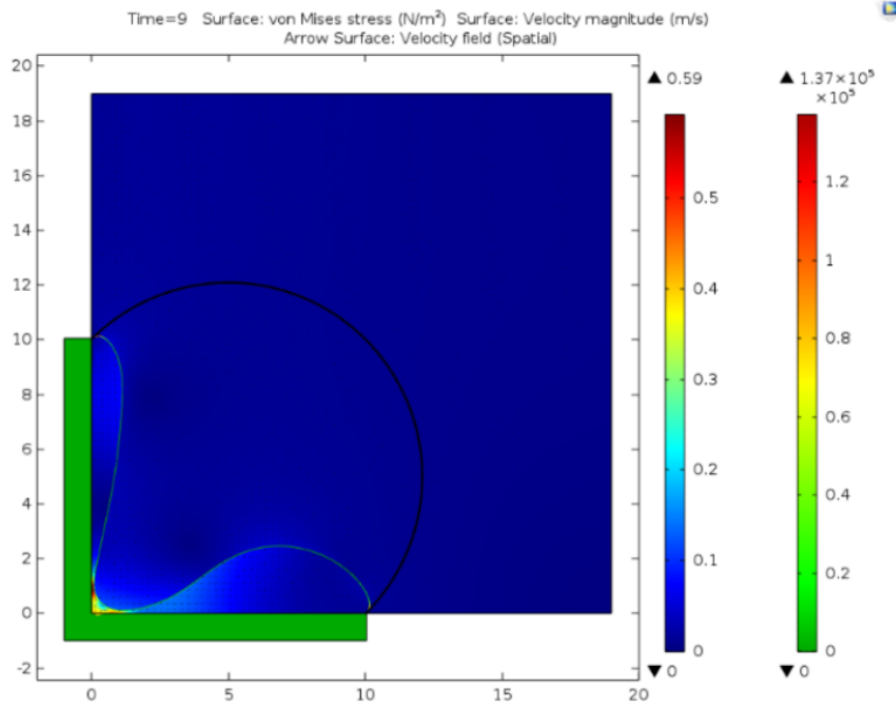


Figure 9: First Comsol simulation of the flexible bladder [7].
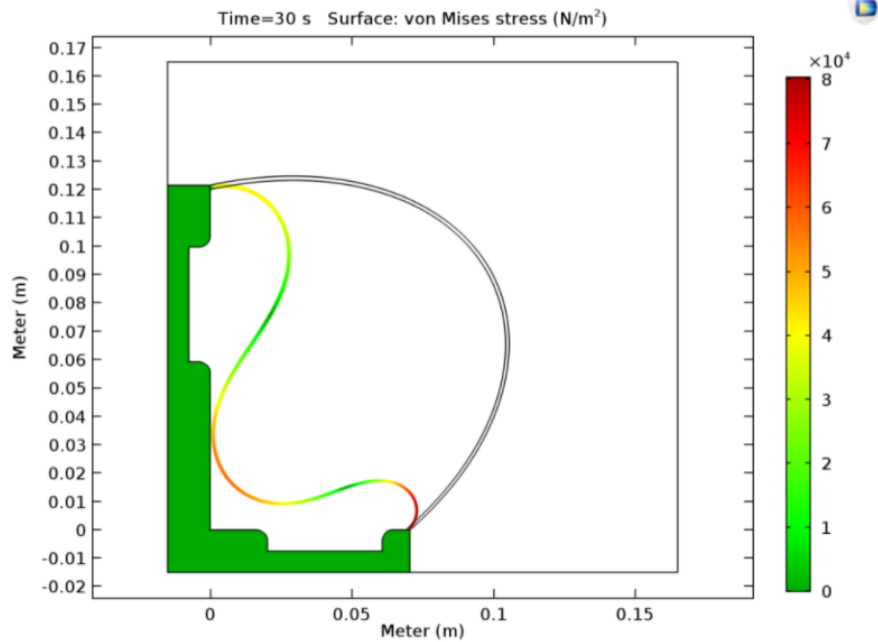
Figure 10: Comsol simulation of the redesigned flexible bladder [8].

In order to overcome the problem the inlet and the outlet were re-designed and new simulations, as shown in figure 10 proved that the deflation process could be preformed without bladder material blocking the outlet [8]. The promising results lead to the decision to create a prototype of the design (figure 11) to further investigate its behaviour during the full inflation/deflation cycle.

Figure 11: Prototype of the redesigned flexible bladder [8].

Validation of the prototype was done using the principles of photogrammetry [9]. During the validation process it appeared that there was much more folding of the bladder material than expected. This is explainable by the fact that the outer-dimension of a circular tube is larger than the inner-dimension which leads to high amount of excessive material in deflated state.
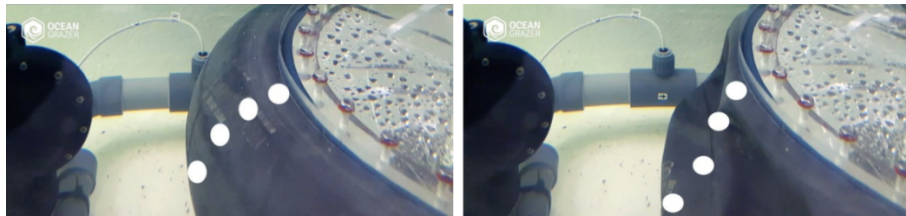


Figure 12: Inflated and deflated state of the prototype [9].

The behaviour and limitations of the prototype lead to the idea of a new design proposed by scientific advisor drs. W.A. Prins. The idea was based on a squared structure that uses caissons for suction to the seabed, and is called the suction design (figure 13).
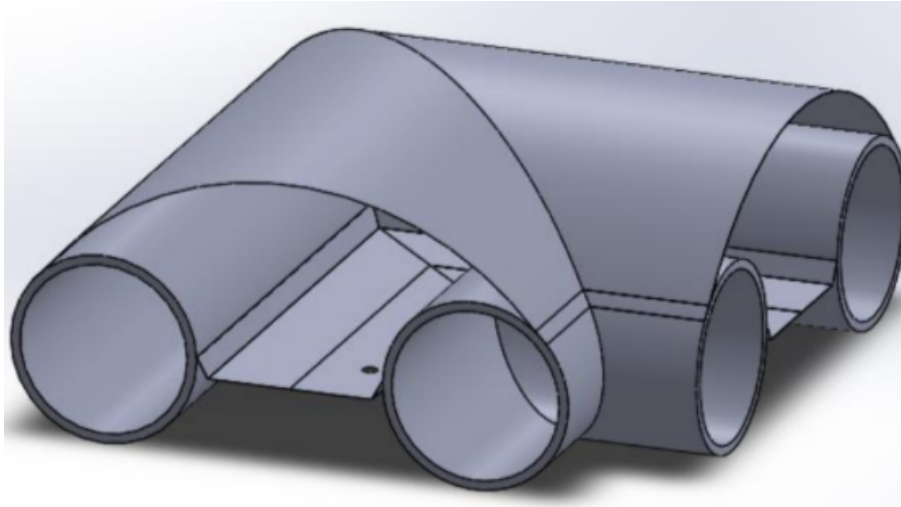
Figure 13: OG battery suction design [10].

The suction design consists out of a rigid reservoir, an engine room and a flexible bladder all in one. According to simulations, the flexible bladder on the squared structure preformed better than that of the circular design with less excessive material and acceptable amount of folding in the middle of the inflation/deflation process, as shown in figure 14 [10].
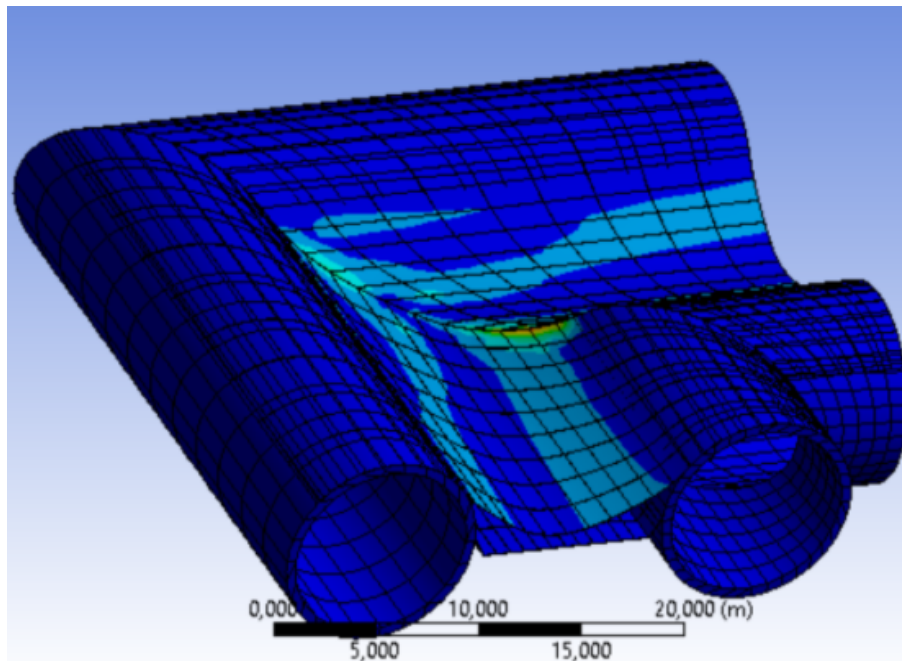


Figure 14: OG battery suction design in deflated condition [10].

**KQ2**: Which existing flexible bladder designs are of interest for the flexible bladder of the OG battery?

The flexible bladder of the OG battery is a liquid storage concept that is completely new. There are no existing designs of flexible bladders that are tested or used under the same shallow water conditions with the idea of a floater and a drain. Therefore, existing flexible bladder designs that are successful in their specific working environment are not applicable to the situation experienced by the flexible bladder of this research. However, strong points of existing designs could be inspirational in the development of the OG battery flexible bladder.

The first shape discussed in literature which is used for underwater air storage is a pumpkin shaped bladder [11]. The idea of the pumpkin is that during inflation the shape becomes almost spherical and during deflation the volume decreases while the design folds along the lines that are typical for the pumpkin shape. Previous research within the OG group determined that this pumpkin shape was not suitable due to problematic excessive material in the deflated condition [9]. Therefore, the design is not of interest in this research.



Figure 15: Pumpkin shaped bladder [11].

The second design is the pillow tank which has not been investigated in previous OG research. However, this design is widely used for transport and storage of liquids [12]. The behaviour of the pillow tank entails that during deflation the sides move outwards while the tank flattens. Therefore, there is almost no folding in the material of the bladder except on the edges (indicated with a white line in figure 16) that move outwards. The difference between the pillow tank and the preliminary design is the large footprint the pillow tank has on the surface whereas the idea of the preliminary design is to have a bladder that floats above the seabed. Furthermore, during inflation/deflation of the pillow tank all the edges have motion in the

same direction, inwards or outwards. With the preliminary design this is not the case since the ends enclosing the preliminary design will have inward movement, while the drain and air tube have outward movement and vice versa.



Figure 16: Pillow tank [12].

The third design mentioned in literature is a bladder tank, which is particularly used for underwater operation [12]. The bladder tank is a flexible tank in a rigid structure to provide support. The bladder is connected to the rigid structure half way the total height of the support structure. In inflated condition the bladder fills the rigid structure, while in deflated condition the bladder floats in the top or lays on the bottom of the rigid structure depend on whether the density of the material is lower or higher than that of the seawater. Folding of the bladder material in fully deflated condition is minimized by the connection to the rigid structure. Downside of the bladder tank design is the large rigid structure that is necessary for the support.
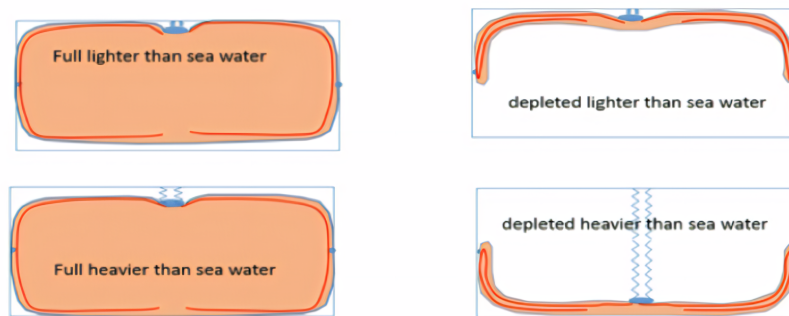


Figure 17: Bladder tank [12].

The fourth design and probably the most appropriate one, in case of the preliminary design, is that of a toothpaste tube. This design has not been used for large flexible bladders yet; however in theory it has the potential to be a solution for the preliminary design. A toothpaste tube is round at one side while being pinned flat at the other end without having folds. The trick of the toothpaste tube is to maintain its circumference along the length of the design [13]. This basically means that at along the shape the width of the tube decreases while the height of

the tube increases. In this manner the round end can be flattened such that is takes on the flattened shape of the other end, with minimal folding. This principle shows great potential as the solution for the ends of the preliminary design.



Figure 18: Toothpaste tube [13]

**KQ3**: Which forces act on the bladder?

The answer to this knowledge question will explain the different forces acting on the bladder. Calculations on the forces will be performed in the treatment design phase (4.1) of this research.

In 3.2.2 the forces acting on the bladder were already briefly mentioned. The first element is the hydro-static pressure, which is based on the amount of water pressing on a structure. The deeper an object is submerged in water the larger the water-column on top of the object becomes. The weight of this water-column in combination with the gravitational force applies a pressure to the bladder.

The second force is the gravitational force which will act on the bladder due to the weight of the whole structure. The interaction between the gravitational force and the buoyancy force will determine whether the bladder sinks or floats.

The third force is the buoyancy force. For this force, the general principle holds that objects submerged in a fluid create a fluid displacement which creates the tendency to float. In combination with the gravitational force the general rule holds that when an object has a higher density than the fluid it is submerged in, it will sink. Vice versa, when an object has a lower density than the fluid it is submerged in, it will float.

As fourth the anchor force is considered. The anchor force is the force on the anchoring points that occur due to the positive difference between the buoyancy force and the gravitational force.

The fourth force is the current force which is applied on the outside of the bladder. Currents are present in the seas and oceans all over the world. The magnitude of the current force on an objects depends on the density of the water, the relevant sea and the shape and size of the object.

The fifth aspect is the pressure of the working fluid acting on the inside of the bladder. When the bladder inflates the pressure of the working fluid is positive, which will lead to expansion of the bladder. When there is no in or outflow of the working fluid the pressure of the working fluid is in a steady-state, such that the bladder maintains its shape. During deflation the back-flow of the working fluid will cause a negative pressure on the inside of the bladder.

**KQ4**: Which aspects are critical during the inflation/deflation process concerning folding of the bladder?

The critical aspect of the design is to provide durability while ensuring performance. The durability of the bladder depends on the cyclic stress and loading in the material. At points where cyclic loading results in repeatable folding the material will crack, which eventually lead to failure [14]. Therefore, it is wishful to reduce to folding to a minimum. On the other hand is is crucial to approach optimal performance of the bladder. In this case of this research it basically means that the bladder should be capable of full inflation and deflation as shown in figure 6.

**KQ5**: Which simulation tool is suitable to simulate the behaviour of the flexible bladder?

For this research multiple simulation software can be used. To extend the research of Kuncorojati the software of Ansys is chosen, since it is the software used during the research on the flexible bladder of the suction design [10]. Ansys is developed for engineering simulations and 3D design, and is able to combine structural and fluent analysis. The software is useful for developing and extending the geometry of the preliminary design followed by simulating the behavior of the, bladder, drain, air tube and flow. In Ansys 3D finite element analysis (FEA) is used to define the deformation and folding of 3D designs. The 3D designs are more of interest than 2D models since 2D models are not able to capture the complexity of the shapes. Therefore, the result of 3D FEA is closer to the situation of an experimental setup than the results of 2D FEA [15].

**KQ6**:What are potential causes for failure of the flexible bladder?

In the development and design of the flexible bladder multiple aspects can lead to failure. To provide a clear visual representation of all aspects that can lead to failure of the performance of the flexible bladder an Ishikawa diagram is constructed. The Ishikawa diagram is a common tool used for cause and effect analysis to identify a complex interplay of causes [16]. The Ishikawa diagram in figure 19 provides a clear overview of all possible causes that can result in an erroneous behaviour of the flexible bladder.
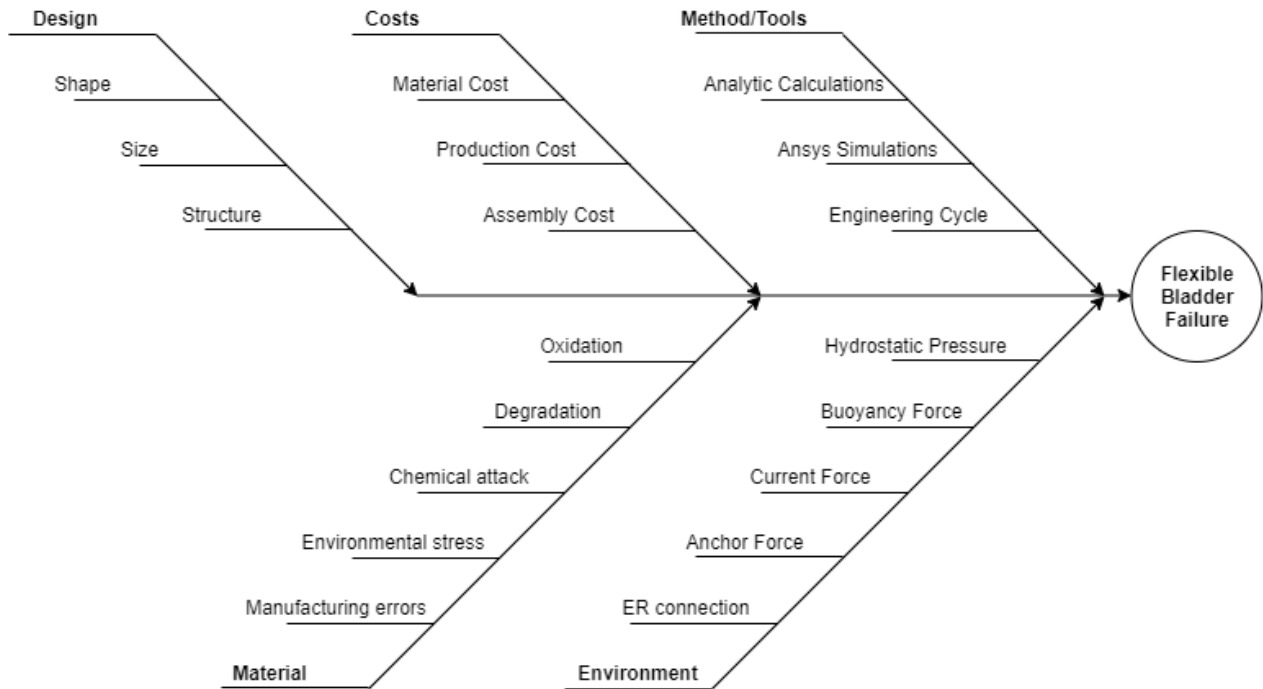
Figure 19: Flexible Bladder Ishikawa Diagram.

The diagram consists of five main categories which are design, costs, method/tools, materials and environment. Failures in the design category can be caused by wrong decision making in shape, size and structure. On the other hand, the three aspects under costs determine if the design is viable. The method/tools category list the tools and methods used in this research and which blundering usage could lead to erroneous outputs. In the category material the main causes for material are failure stated and need to be taken in consideration when choosing the bladder material and supportive structure [17]. In the fifth category, environment, the forces due to the specific external conditions that can lead to failures are itemized. During this research the main focus is on the design category taking into consideration the material, environment and method/tools category. The cost category is not be further discussed in this research.

# 4 Treatment Design

## 4.1 Requirements and Design Questions

In the Treatment Design phase of the research requirements and design questions are formulated to acquire guidance for the development of the design

**DQ1**: What are the requirements for the flexible bladder design?

The requirements for the flexible bladder are set by the OG B.V. and are based on the capa-

bilities the flexible bladder should have. The first requirement is based on the desired energy capacity, which should have a minimum of 1 megawatt-hour. The desired energy capacity is the starting point on which the dimensions of the bladder will be based on. The second requirement is based on durability of the material and this insists to approach minimal folding. The less folding occurs during inflation/deflation, the longer the lifetime of the material will be [14]. The third requirement entails that the flexible bladder must float above the seabed such that there is no risk of dune formation against the bladder, and that a strong undertow that occurs in seas and oceans can flow between the seabed and the bladder [18]. The fourth requirement is that the bladder should be capable of withstanding the external forces such as gravity, hydro-static pressure and current force. The fifth and sixth requirement are based on requirements set by the OG BV and concern the inflation and deflation time. The time span set for inflation of the bladder is between two and four hours. The deflation time is set at a time span of half an hour. The last requirement entails that there should be a connection between the flexible bladder and the engine room such that the working fluid is able to flow from and to the engine room.

**DQ2**: What are the constant parameters that need to be taking into account for the flexible bladder design?

For this research there are two assumptions made in order to provide constant values for required calculations. The first constant is that the seabed is at 30 meter below the surface of the sea. The second constant is based on the depth of the rigid reservoir. For this research there rigid reservoir is assumed to be at a depth of 50 meters below the seabed which leads to a pressure head of 80 meters.

**DQ3**: What are the variables that need to be taking into account for the flexible bladder design?

The variables in this research are the factors that have an impact on the flexible bladder behavior and require a decision in order to achieve the requirements that are set. The first variable is the bladder size, since the capacity is set as a requirement it can be used to calculate the total volume of the bladder. This total volume can be achieved by one large bladder, or by multiple smaller ones. Secondly, the thickness of the material can be shifted to create a bladder that is not thicker than necessary, although it can withstand the loads exerted. The third variable is the material type. In previous research on flexible bladders within the OG research group Ethylene propylene diene monomer (EPDM) was used as membrane material. The material was found to be suitable based on its performance in water and its abrasive resistance due to its mechanical and chemical properties stated in Appendix A [19]. Furthermore, the first experimental model of the flexible bladder was made out of EPDM showing no significant material problems. Moreover, the material is dependent on the available materials within the simulation software. EPDM is a rubber-like material and rubber is a material available within

the simulation software which can be tuned to have the appropriate density and isotropic elasticity. The fourth variable is the shape of the bladder itself, because the shape is crucial during the inflation/deflation process and has high influence on the amount of folding. As fifth the variable structure is taken into consideration. Adding a structure can be necessary for providing support or additional strength to the shape and material chosen for the design. The sixth variable is the tube dimension which depends on the bladder size and thus the amount of bladders. Variable seven is the inflow and outflow which can be controlled by the velocity of the flow.

| Constant parameters | Requirements | Variables |
|---|---|---|
| (1) Hydrostatic pressure at 30m seabed depth | (1) Capacity of 1MWh | (1) Bladder size |
| (2) Pressure head of 80m | (2) Minimal folding | (2) Bladder thickness |
| | (3) Floating | (3) Material type |
| | (4) Withstand forces | (4) Shape |
| | (5) Inflation time 2h-4h | (5) Structure |
| | (6) Deflation time 0.5h | (6) Tube dimension |
| | (7) ER connection | (7) In/outflow |
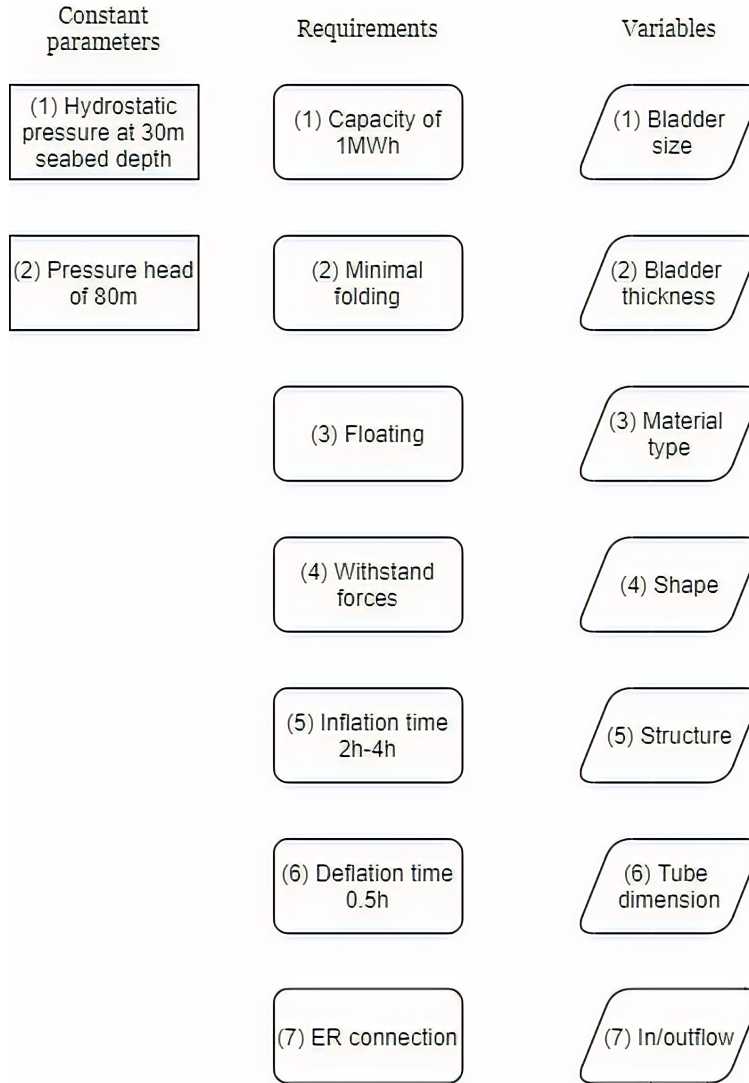
Figure 20: Constant parameters, requirements and variables

**DQ4**: What is the required total volume of the working fluid?

In order to calculate the total volume ($V_{max}$) of the bladder, the required energy capacity ($E_{max}$) is taken as a starting point. The capacity is multiplied with 3600 and subtracted by

the turbine efficiency ($\mu$) multiplied by the pressure difference ($\Delta p$) due to the pressure head of 80 meters. This results in a required total volume of 5625 cubic meters.

$$V_{max} = \frac{3600 E_{max}}{\Delta p \mu} \tag{1}$$

Table 1: Total volume variables

| Variable | Value | Unit |
|----------|-------|------|
| $\mu$ | 0.8 | $-$ |
| $\Delta p$ | 800 | $kPa$ |
| $E_{max}$ | 1 | $MWh$ |
| $V_{max}$ | 5625 | $m^3$ |

**DQ5**: Which dimension should the inlet/outlet have?

Based on the total volume and the desired deflation time the discharge rate ($Q_d$), diameter of the inlet/outlet ($D_p$), and flow velocity ($v$) can be calculated. It becomes clear that the inlet, outlet should have a diameter of 1.27 meters and that the flow velocity should be 2.46 meters per second to accomplish a discharge rate of 3.13 cubic meters per second.

$$Q_D = \frac{V_{max}}{t_D} = Av \tag{2a}$$

$$D_p = 0.72\sqrt{Q_D} \tag{2b}$$

$$A = (\frac{1}{2}D_p)^2 \pi \tag{2c}$$

Table 2: Inlet/outlet dimension variables

| Variable | Value | Unit |
|----------|-------|------|
| $V_{max}$ | 5625 | $m^3$ |
| $t_D$ | 1800 | $s$ |
| $Q_D$ | 3.13 | $m^3/s$ |
| $D_p$ | 1.27 | $m$ |
| $A$ | 1.27 | $m^2$ |
| $v$ | 2.46 | $m/s$ |

**DQ6**: What is the magnitude of the forces that act on the bladder?

**Hydro-static pressure**

The hydro-static pressure is calculated by first multiplying the height of the water column on top of the bladder with the density of seawater ($\rho_{sw}$) and the gravitational constant and adding the atmospheric pressure. The outcome is the total pressure exerted on the bladder due to the weight of the seawater.

$$P_{hydro} = \rho_{sw}gh + P_{Atm} \tag{3}$$

Table 3: Hydro-static pressure variables

| Variable | Value | Unit |
|----------|-------|------|
| $\rho_{sw}$ | 1025 | $kg/m^3$ |
| $g$ | 9.81 | $m/s^2$ |
| $h$ | 30 | $m$ |
| $P_{atm}$ | 100 | $kPa$ |
| $P_{hydro}$ | 401.7 | $kPa$ |

**Gravitational Force**

The gravitational force on the bladder is calculated by taking the total weight of the bladder and multiplying it with the gravitational constant. The total weight of the bladder is calculated by taking the volume of each part of the bladder and multiplying it with its corresponding density. The parts of the bladder are the bladder material, the air tube, the drain material and the working fluid.

$$F_g = (V_b\rho_b + V_a\rho_a + V_d\rho_d + V_{wf}\rho_{wf})g \tag{4}$$

**Buoyancy force**

The buoyancy force is a force based on the tendency of an object to float due to difference in density with the liquid they are submerged in. To calculate the buoyancy force, the total water displacement is considered by summing the volumes of the different parts of the flexible and multiplying this number with the density of seawater ($\rho_{sw}$) and the gravitational constant.

$$F_b = (V_b + V_a + V_d + V_{wf})\rho_{sw}g \tag{5}$$

**Anchor force**

Since the bladder is supposed to float above the seabed, the buoyancy force must be higher than the gravitational force. The sum of both forces will be the forces exerted on the anchor

that keeps the bladder in place. In order to achieve a buoyancy force that is higher than the gravitational force, the air tube must be of a certain size such that the air-volume can carry the weight of the structure. For the calculations of the air-volume a few assumptions are made. The first assumption is the bladder thickness, previous research on the flexible bladder stated that 15 millimeters of wall thickness is an appropriate value [10]. Therefore, in these global calculations the wall thickness will be for the bladder, air tube and drain will be 15 millimeters. Furthermore, to approximately calculate the volume of the bladder material a cylindrical bladder with a diameter of 10 meters and a length of 75 meters is assumed which will achieve the desired total volume. Creating such a design with a wall thickness of 15 millimeters results in a bladder material volume ($V_b$) of 35.40 cubic meters. Based on the diameter of the inlet/outlet calculated in design question 5 the volume of the drain material can be calculated. Since the upper halve of the drain is pinched such that working fluid can flow in- and out the drain, an eight of the total volume is subtracted. This results in a total drain volume ($V_d$) of 4.54 cubic meters. Adding the known values for the total volume of the working fluid ($V_max$), the density of the working fluid ($\rho_{wf}$), the density of the bladder material ($\rho_b$, the density of the drain material ($\rho_d$), the density of seawater ($\rho_{sw}$), the density of air ($\rho_a$) and the gravitational constant and inserting them in a combination of equation 4 and 6 it is possible to calculate the volume of air necessary to keep the whole structure float. Since the density of the working fluid is lower than the density of seawater it causes extra flotation. Therefore, in equation 6d the influence of the working fluid is deleted to cover the deflated condition. This results in an air-volume of 40.37 cubic meters required to keep the structure floating.

$$\sum F = F_b - F_g = 0 \tag{6a}$$

$$F_b = F_g \tag{6b}$$

$$(V_b + V_a + V_d + V_{max})\rho_{sw}g = (V_b\rho_b + V_a\rho_a + V_d\rho_d + V_{max}\rho_{wf})g \tag{6c}$$

$$(V_b + V_a + V_d)\rho_{sw}g = (V_b\rho_b + V_a\rho_a + V_d\rho_d)g \tag{6d}$$

Table 4: Anchor force variables

| Variable | Value | Unit |
|----------|-------|------|
| $g$ | 9.81 | $m^{s2}$ |
| $V_{max}$ | 5625 | $m^3$ |
| $\rho_{wf}$ | 1000 | $kg/m^3$ |
| $V_b$ | 35.40 | $m^3$ |
| $\rho_b$ | 1330 | $kg/m^3$ |
| $V_d$ | 4.54 | $m^3$ |
| $\rho_d$ | 7750 | $kg/m^3$ |
| $\rho_{sw}$ | 1025 | $kg/m^3$ |
| $V_a$ | 40.37 | $m^3$ |
| $\rho_a$ | 1.225 | $kg/m^3$ |

Additionally, the total gravitational and total buoyancy force for this steady-state can be calculated for inflated and deflated condition now the air volume is known using equation 4 and 6.

Table 5: Gravitational/buoyancy force variables

| Variable | Value | Unit |
|----------|-------|------|
| $F_g/F_b(inflated)$ | 57 | $MN$ |
| $F_g/F_b(deflated)$ | 808 | $kN$ |

**Current force**

Objects in oceans or seas are exposed to the forces of the current. The current force is determined by the density and the current velocity of the particular sea in combination with the dimension of the object exposed to the current [20]. The velocity of the current in the north sea varies between 0.02 and 0.67 meter per second depending on the exact location [21]. Furthermore, which side of the bladder is facing the current is crucial since the smaller the contact area ($A$) of the object facing the current, the lower the current force will be. Moreover, the shape of the side facing the current is very important, since the more aqua-dynamic the object is, the lower the drag coefficient ($C_d$) which is directly related to the magnitude of the current force.

$$F_{current} = \frac{1}{2}\rho_{sw}v^2C_DA \qquad (7)$$

Table 6: Current force variables

| Variable | Value | Unit |
|---|---|---|
| $\rho_{sw}$ | 1025 | $kg/m^3$ |
| $v$ | $0.02 \sim 0.67$ | $m/s$ |
| $C_d$ | shape dependent | – |
| $A$ | size dependent | $m^2$ |

**Pressure of the working fluid**

During steady-state inflated condition there is no pressure change within the bladder due to the working fluid. At the moment the bladder starts deflating, a pressure drop occurs within the bladder by cause of the outflow of the working fluid. The rigid reservoir is under atmospheric pressure as a result of an umbilical cord connected to the surface of the sea. Furthermore, the rigid reservoir is placed 50 meters beneath the seabed, which is at a depth of 30 meters, causing a pressure head of 80 meters. Additionally, the diameter of the inlet/outlet as well as the flow velocity are calculated in equation 2. Inserting these values in the Bernoulli equation leads to the calculation of the pressure difference in the bladder [22].

$$p_1 + 0.5\rho v_1^2 + \rho g h_1 = p_2 + 0.5\rho v_2^2 + \rho g h_2 \tag{8a}$$

$$p_1 - p_2 = 0.5\rho(v_2^2 - v_1^2) + \rho g(h_2 - h_1) = \Delta p \tag{8b}$$

Table 7: Working fluid pressure variables

| Variable | Value | Unit |
|---|---|---|
| $\rho_{wf}$ | 1000 | $kg/m^3$ |
| $v$ | 2.46 | $m/s$ |
| $g$ | 9.81 | $m/s^2$ |
| $h_1$ | 80 | $m$ |
| $h_2$ | 0 | $m$ |
| $\Delta p$ | 784.8 | $kPa$ |

## 4.2 Simulation designs and tools

### 4.2.1 Designs

In order to approve or disapprove certain design decisions, multiple designs will be tested on their functionality. The first design that will be tested is the preliminary design without caps closing the

end. The simulations of this very simplistic design will indicate whether the basic idea of a fixed drain and a vertical moving air tube will stretch the material, such that the folding during deflation is brought to a minimum.

Subsequently, the ends will be closed with round shaped caps. In theory the round shaped caps provide abundant material to cover the vertical movement of the air tube without elastic behaviour. Disadvantage is the abundant material in horizontal direction which theoretically leads to excessive material and folds when transforming to the deflated shape.

Thereafter, the round caps are modified such that a pumpkin shape occurs. In the design of the pumpkin shape, the round cap is replaced with multiple smaller faces that have a curved pointy shape. The idea is that the firmness of the solid round caps is breached and that folding occurs along the edges of the connected pointy faces. Theoretically, the problem that occurs at the rounded caps is still existing at this pumpkin shaped caps, since there is excessive material in the horizontal direction. However, it is interesting to see whether the folding lines give rise to unequal deformation compared to the round caps.

The final design that will be tested is the toothpaste tube shaped caps. The toothpaste tube shaped caps have an unique form in which the outer ends already embrace the desired deflated shape whilst being in the inflated condition. This principle is achieved by designing a narrow profile that has a circumference identical to inflated rounded body of the preliminary design with the diameter equal to the air tube and drain. Creating a smooth blend between both creates the typical toothpaste tube shape. In theory, the round shape deforms towards the narrow oblong shape without folding or excessive material.

### 4.2.2  Transient structural

Transient structural analysis is a method within Ansys used to determine the dynamic response of the bladder over time. The transient structural analysis enables the possibility to capture time-dependent results such as displacement, stress, strain and reaction force of the bladder under influence of steady-state loads and transient loads. Transient structural has the advantage that it considers inertia and damping effects, on the other hand is has the disadvantage that is requires high amount of computational time and memory. The equation of motion Ansys uses for the transient structural analysis is:

$$M\frac{d^2u}{dt^2} + C\frac{du}{dt} + Ku = F(t), \tag{9}$$

where $(M)$ is the mass matrix, $(C)$ is the damping matrix, $(K)$ is the stiffness matrix, $(\frac{d^2u}{dt^2})$ is the nodal acceleration $(\frac{du}{dt})$ is the nodal speed, $(u)$ is the nodal displacement and $(F)$ is the load at any given time. The ANSYS program uses the New-mark time integration method to solve these equations at discrete time-points [23]. The New-mark method allows the direct solution of a second-order differential equation or a system of second-order differential equations without the need

for the transformation to a pair of simultaneous first-order differential equations [24]. The solver transient structural analysis in Ansys utilizes for the mesh is the Mechanical Ansys Parametric Designs Language (MAPDL) solver.

During the simulations in transient structural analysis the large deflection setting is enabled. Setting large deflection to on will take into account stiffness changes resulting from change in element shape and orientation due to large deflection, large rotation, and large strain. The enabling of large deformation will lead to more accurate results. However, it requires an iterative solution and loads to be applied in smaller steps which lead to a longer solving time. Hence, the iterative solver within Ansys is used for the simulations.

### 4.2.3 Fluent

In order to capture the influence of the flow of the working fluid, Ansys Fluent is used to define the volume of the working fluid, the position of the outflow and the pressure present in the outflow. Ansys fluent utilizes a Computation Fluid Dynamics (CFD) solver for its calculations which are transferred to the transient structural part, wherefore the incorporation of the working fluid pressure on the inside of the bladder walls is enabled. In this manner one-way-fluid structure interaction (FSI) is accomplished. As depicted in figure 21 the fluid behaviour is determined over time and linked to the transient structure analysis in order to simulate the effect of the fluid on the bladder. Influence of structure analysis on the fluid is neglected in this type of FSI.
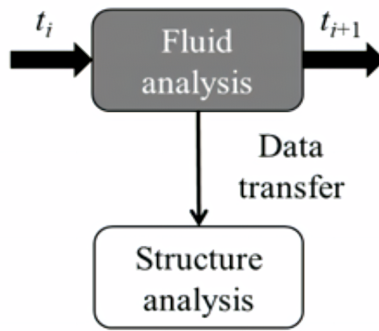


Figure 21: One-way-FSI [25]

### 4.2.4 Material properties

Based on the positive results in previous research EPDM is chosen as bladder material in this research. Rubber is available within the material database of Ansys, although it requires additional data input to be functional as EPDM. Literature on the density of EPDM shows some degree of variation; however in this research the density is set at 1330 kilograms per cubic meter [26]. Furthermore, in Ansys the isotropic elasticity of the material is based on the Young's modulus and the Poisson's ratio which are set at 6 megapascal and 0.5 approximately [27] [28]. The air tube,

drain and solid end caps are made out of structural steel which is a material preset in the material database of Ansys. In Ansys structural steel has a density of 7850 kilograms per cubic meter, a Young's modulus of $2e5$ megapascal and a Poisson's ratio of 0.3. The Young's modulus is based on the linear section of the strain-stress curve of a material and is calculated by:

$$E = \frac{\sigma}{\epsilon}, \tag{10}$$

where $E$ is the Young's modulus in $\sigma$ is the stress rate in mega-pascals and $\epsilon$ is the strain rate in millimeter/millimeters [29]. Basically, the Young's modulus is a mechanical property that indicates the stiffness of a material. The higher the Young's modulus, the stiffer the material and the less it will deform under certain stress.

The Poisson's ratio is based on the amount of longitudinal elongation in comparison with the lateral contraction and is calculated by:

$$v = -\frac{\epsilon_{lateral}}{\epsilon_{longitudinal}}, \tag{11}$$

where $v$ is the dimensionless Poisson's ratio, $\epsilon_{lateral}$ is the lateral contraction of the material in millimeters/millimeters and $\epsilon_{longitudinal}$ is the longitudinal elongation of the material in millimeters/millimeters [29]. The general idea of the Poisson's ratio is that it describes in which ratio a material gets narrower while being stretched.

### 4.2.5 Boundary conditions

Due to the lack of computational power the designs are scaled to one thousand of the full scale size in order to accomplish simulations on the different designs without computational errors. The same scaling ratio is used on the forces and pressures to ensure adequate simulations. Equation 6 indicates that gravitational force and buoyancy force are supposed to be equal in order to maintain the vertical (Z-axis) position of the bladder. Therefore the gravitational force is cancelled in the simulation and the buoyancy force applied is the extra buoyancy force required to induce deformation of the bladder. The hydro-static pressure calculated with equation 3 is scaled according to the scaling ratio which implies a pressure of 0.4 pascal on top op the bladder (-Z-direction). Furthermore, in the simulations all designs have the common factor that they have a drain and an air tube. Both the drain as the air tube are designed as solid round bars of structural steel to prevent extensive bending. In the simulations the drain is always addressed as fixed support whereas on the air tube is always under exertion of a buoyancy force of 0.25 millinewton (Z-direction). Moreover, the drain and are tube are always partly restricted in their freedom of displacement. They are free to displace in vertical direction (Z-direction) and free to elongate (Y-direction), while being restricted to move sideways (X-direction). The thickness of the bladder material is 0.015 millimeters according to the scaling ratio and the 15 millimeters thickness used in previous research [10]. The design that performs best is elaborated with one-way-FSI that entails a gauge pressure of 0.8 pascal deduced by scaling the

pressure that is calculated with equation 8.

Table 8: Boundary conditions

| Boundary | Value | Unit |
|---|---|---|
| Bladder thickness | 0.015 | mm |
| Drain | Fixed | - |
| Air tube | 0.25 | mN |
| Hydrostatic pressure | 0.4 | Pa |
| | | |
| Displacement: | | |
| X | 0 | mm |
| Y | Free | - |
| Z | Free | - |
| | | |
| Outflow: | | |
| Gauge Pressure | 0.8 | Pa |

### 4.2.6 Strain

Ideally the bladder deforms from the inflated state to the deflated state without folding or elongation of the bladder material. In order to indicate the amount of elongation strain analysis is applied on the solution of the simulation. Strain is based on the length of the structure after deformation in comparison to the length of the structure before deformation, which lead to the basic equation of strain:

$$\epsilon_e = \frac{\Delta L}{L_0}, \tag{12}$$

where $\epsilon_e$ is the strain, $\Delta L$ is the elongation in meters and $L_0$ is the original length in meters [29]. However, the simulations in this research are 3D based and therefore, equivalent von Mises strain is used to calculated strain taking in consideration the X, Y and Z direction of the design. The equivalent von Mises strain in Ansys is calculated using the following equation:

$$\epsilon_e = \frac{1}{1+v}(\frac{1}{2}[(\epsilon_1 - \epsilon_2)^2 + (\epsilon_2 - \epsilon_3)^2 + (\epsilon_3 - \epsilon_1)^2])^{\frac{1}{2}}, \tag{13}$$

where $\epsilon_e$ is the equivalent von Mises strain, $v$ is the Poisson's ratio of the material and $\epsilon_1$, $\epsilon_2$ and $\epsilon_3$ are the strains in the three different directions of the 3D simulation.

# 5 Treatment validation

## 5.1 Without caps

Starting with a circular body with a diameter of 10 millimeters that contains two tubes, one as the air tube and one as the drain, the preliminary design is tested to detect whether the theory of an air tube that lifts the body and stretches the material in order to prevent folding holds. The starting shape of the simulation is depicted in figure 22.
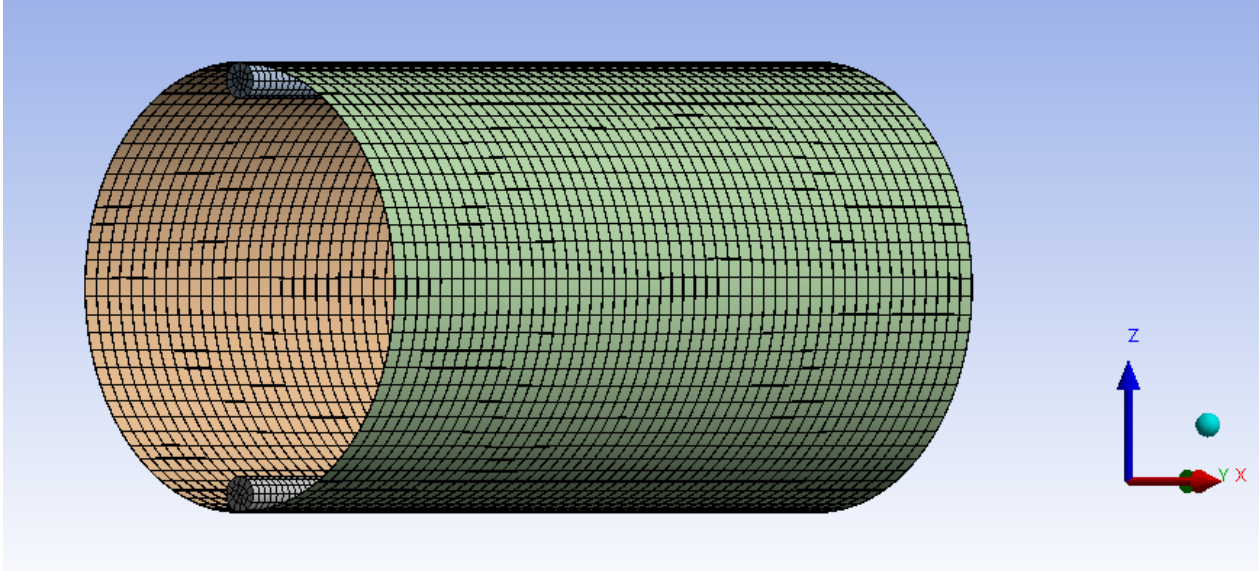


Figure 22: Inflated preliminary design without caps

After applying the buoyancy force of 0.25 millinewton on the air tube the bladder start deforming in horizontal and vertical direction. The air tube stretches the material without folding, whereas the sidewalls move inwards. Therefore, the volume of the bladder decreases, which is according to the principle of the deflating bladder that contains preferably no working fluid at its final state. However, full deflation is hard to achieve since the bladder material tends to elongate which becomes more clear when focusing on the strain analysis. The equivalent elastic strain analysis indicates that the strain occurs at the contact points between air tube/drain and the bladder.
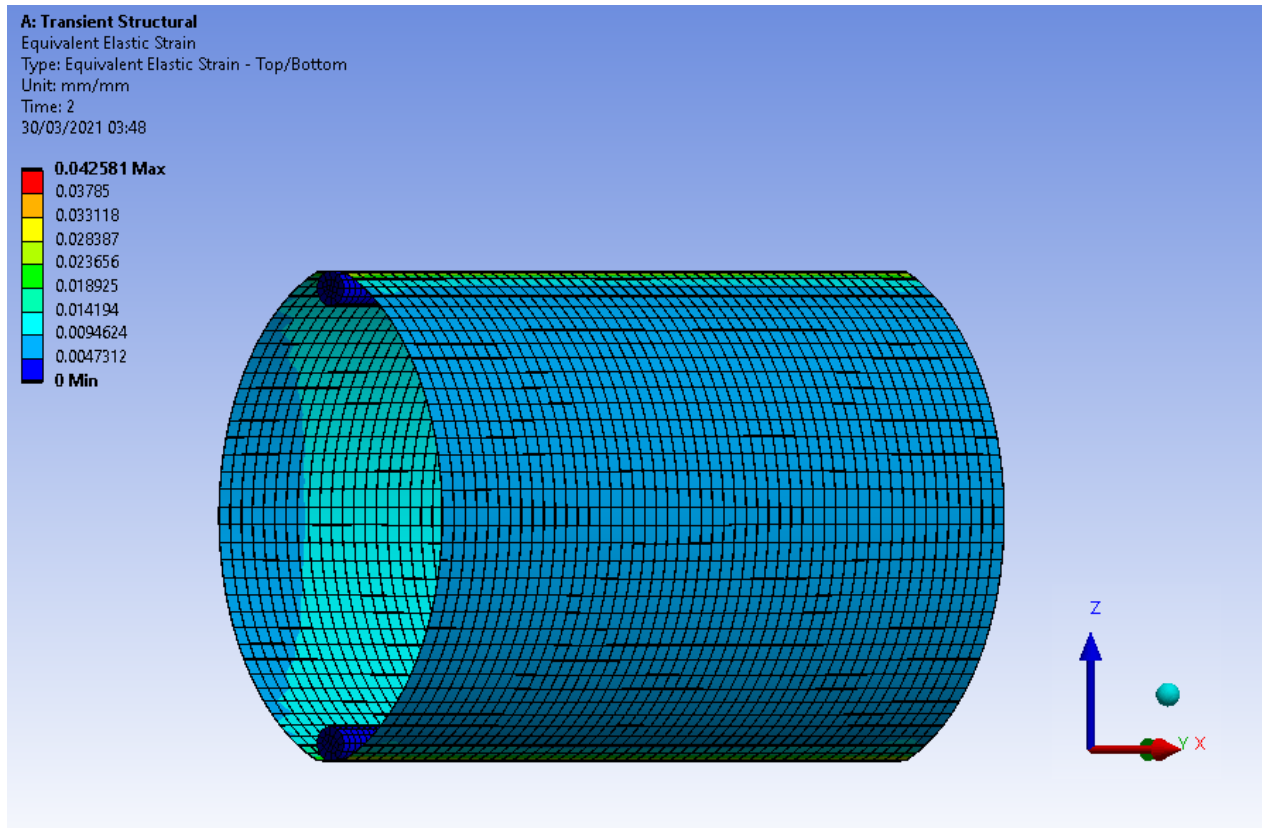
Figure 23: Deflated preliminary design without caps

## 5.2 Round caps

The preliminary design with round caps closing the ends has the advantage that due to the abundant material in the Z-direction the bladder can stretch vertically without causing any strain. On the other hand, the horizontally inward movement of the bladder leads to excessive material that needs to folds in order to convert the round shape to an oval shape. The starting shape is depicted in figure 24. The element size used for the mesh is 0.8 millimeters with refinements of 0.2 millimeters on the end caps itself.
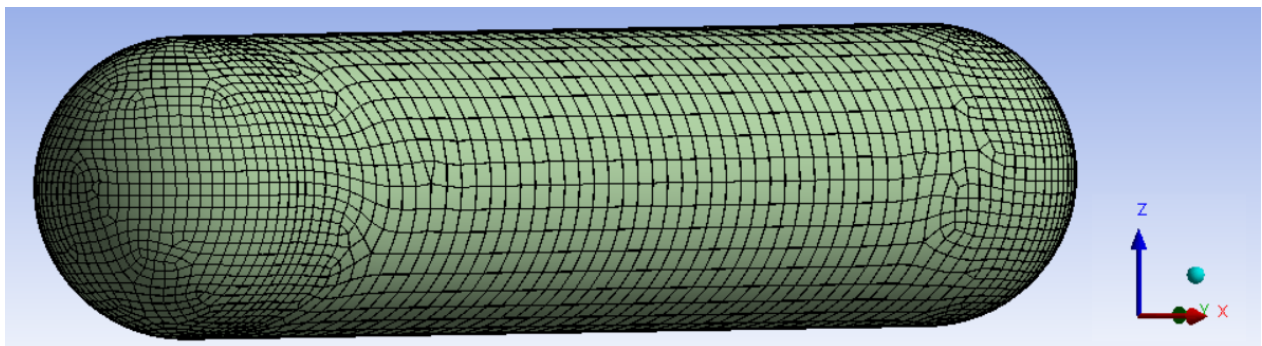


Figure 24: Inflated preliminary design round caps.

Exercising the buoyancy force of 0.25 millinewton on the air tube result in different deformation than thought on forehand as can been seen in figure 25. Obviously the round caps sides provide firmness to the structure on both ends whereby there is no folding and almost no deformation at the end caps. Furthermore, it leads to a bulge covering the side of the bladder. The equivalent elastic strain analysis shows that there is maximum strain of $1.5e-3$ millimeter/millimeter at the point the air tube and drain have contact with the bladder. This indicates that the material elongates at the contact points, which is undesirable.
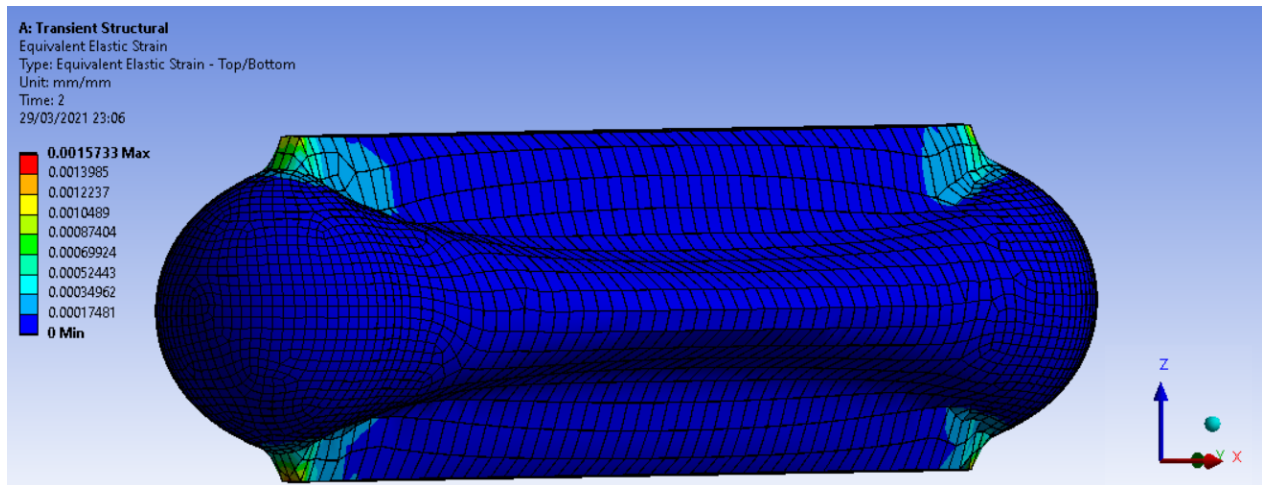


Figure 25: Deflated preliminary design round caps

## 5.3 Pumpkin caps

The pumpkin caps are not as spherical as the round caps. The caps are a merge of multiple slightly curved point-shaped faces. The edges of the faces provide folding lines in order to breach the solidity the round caps gave to the design. The inflated starting shape is shown in figure 26, the mesh has general element size of 0.8 millimeters is used, while the pumpkin caps are refined with a element size of 0.2 millimeters.
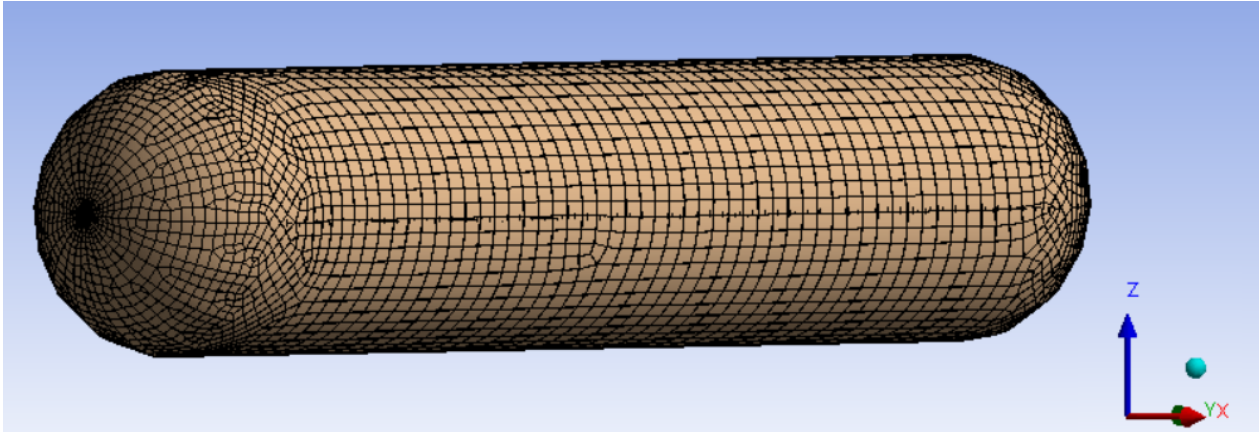
Figure 26: Inflated preliminary design with pumpkin shaped caps

The simulation shows that the folding lines do not have a significant impact on the deformation of the bladder, as shown in figure 27. There is still a bulge on the side of the bladder; however the bulge has become smaller. Moreover, the equivalent elastic strain analysis indicate that there is more strain at the contact points of the air tube/drain and bladder in comparison to the round ends with a maximum of $8.5e-3$ millimeter/millimeters. Hence, the pumpkin shaped end caps still provide to much support and can not prevent the elongation of the bladder material at the contact points.
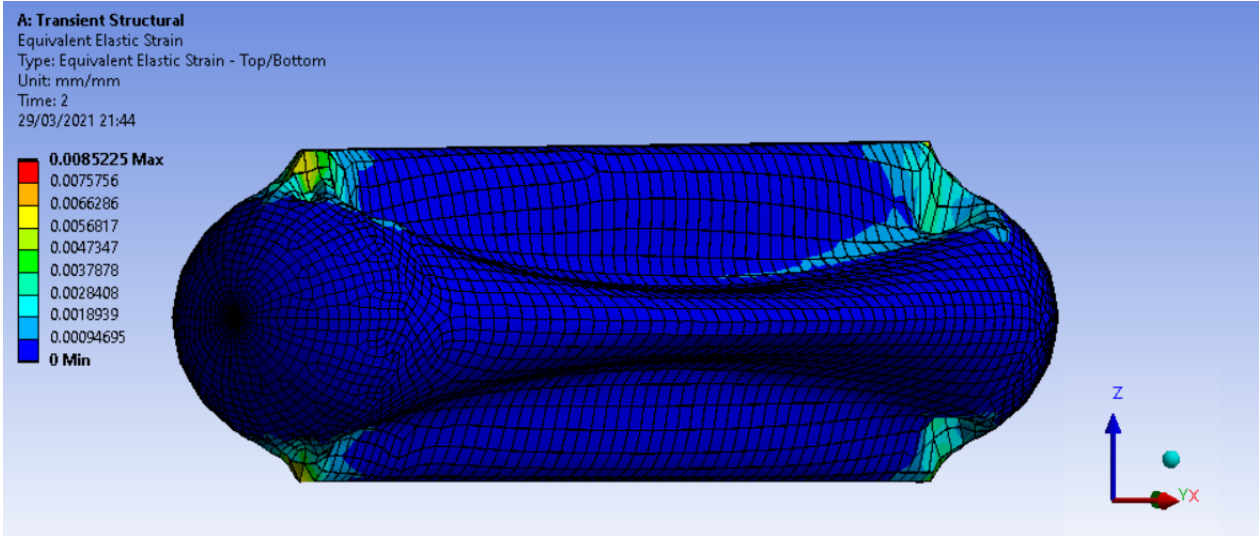


Figure 27: Deflated preliminary design with pumpkin shaped caps

## 5.4 Toothpaste tube caps

In order to demonstrate the behaviour of the toothpaste tube end caps a cross section of the design is simulated first. The cross section in figure 28 shows how the end of the bladder is perfectly round while the other end is a rounded oblong solid having a width equal to the diameter of the air

tube/drain. The circumference of the bladder is equal over the blend between the two shapes whereby in theory the round end can transform to the shape of the rounded oblong solid without folding or elongation of the bladder material. The general mesh size is 0.4 millimeters, with refinements of 0.2 millimeters at the spines at which the air tube/drain make contact with the bladder. This simulation has a slight difference in boundary condition compared to the other simulations. In this case a force is exerted on the air tube and drain in opposite direction with a magnitude of 0.125 newton while the solid end caps is a fixed support.
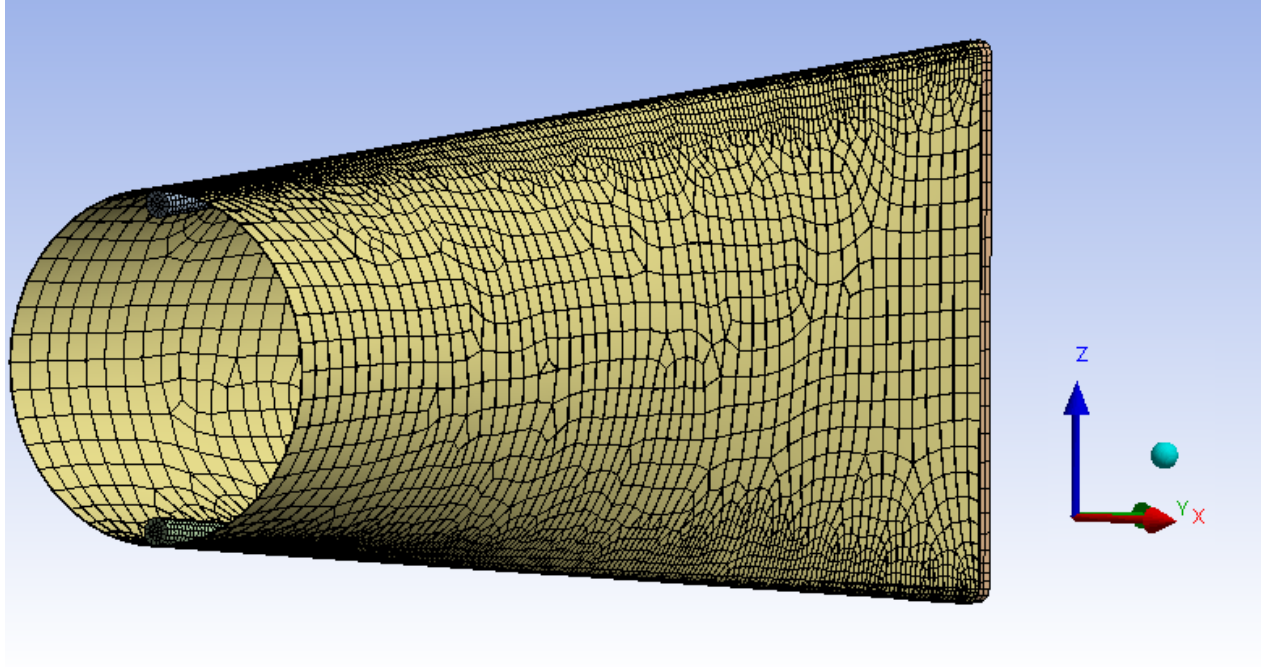


Figure 28: Inflated preliminary design with toothpaste tube shaped cap

The simulation of the cross section of the toothpaste tube capped design in figure 29 shows that the design can deform without folding while reducing the volume on the inside of the bladder. A risk that occurs is that the side walls at the flattened end of the cap make contact while the walls at the round end side are still deforming to the desired deflated shape. This can cause working fluid to be trapped in the upper part of the bladder. Another aspect that stands out is that there is still quite some space between the sidewalls at the open end while the distance between the wall should be minimal based on the geometry of the design. This could indicate that the small amount of strain in the material negatively influences the deformation, since the circumference of the bladder is not equal anymore at every point of the bladder.
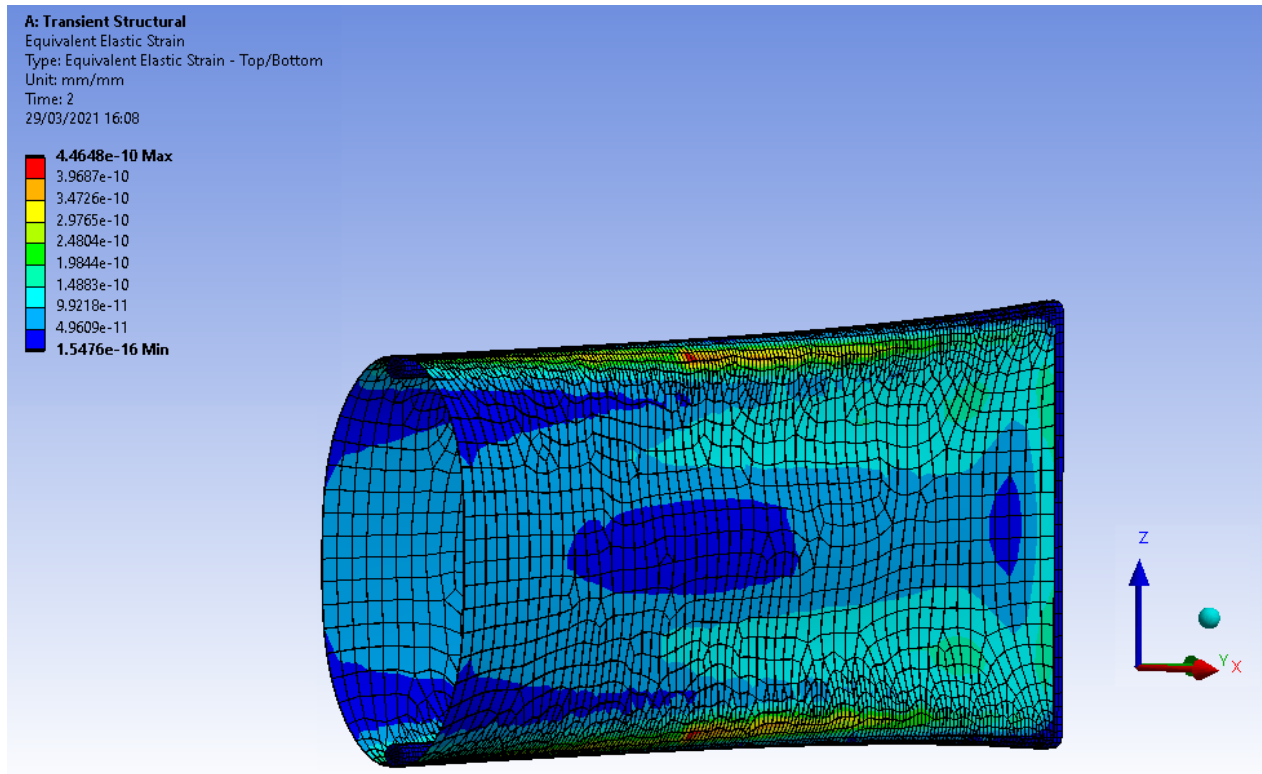
Figure 29: Deflated preliminary design with toothpaste tube shaped cap

To further examine the toothpaste tube shape the cross section is elaborated to a full bladder with two toothpaste tube caps enclosing the bladder. The side- and top view of the full bladder are depicted in figure 30. The design consists out of two toothpaste tube end caps connected by a round tube. Furthermore, a outlet is designed in the drain to enable the simulation of the one-way-FSI. The gauge pressure of the inlet is a scaled version of the pressure calculated in equation 8 and is set at 0.8 Pascals. The equally distributed pressure over the outlet and bladder is displayed in figure 31. The element size used for the mesh is 0.8 millimeters for the circular midsection, 0.4 millimeters for the flanks of the toothpaste tube caps and 0.2 millimeters for the spines of the toothpaste tube caps.
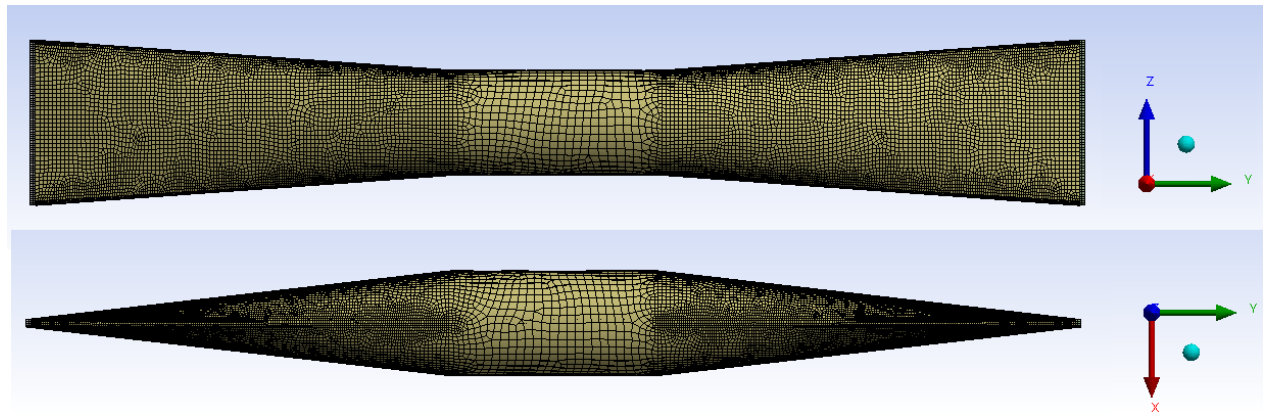
Figure 30: Side -and top view of the inflated preliminary design with toothpaste tube shaped caps at both ends
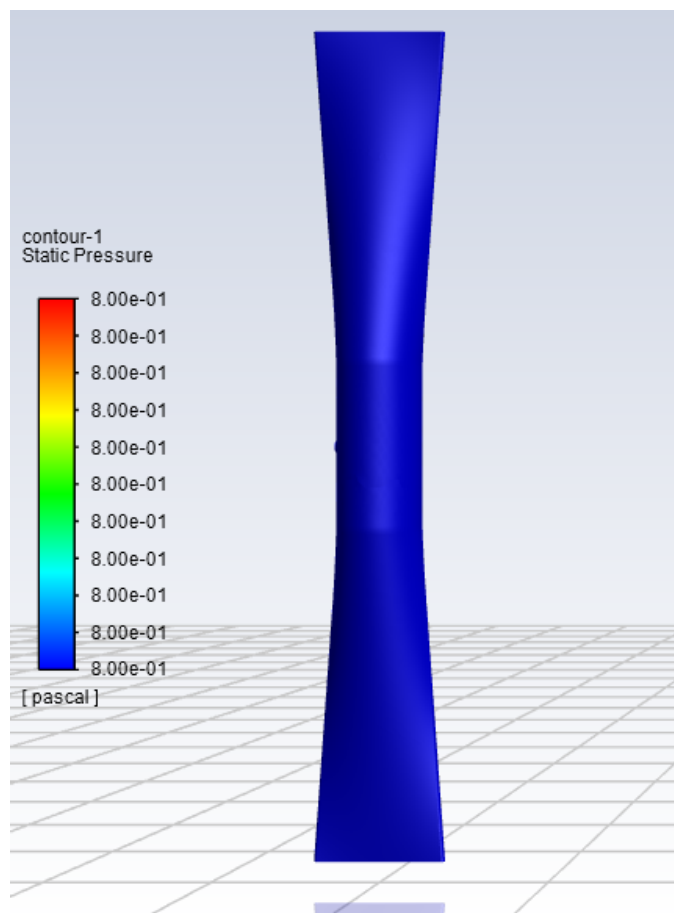


Figure 31: Pressure distribution over the bladder wall

The outcome of the simulation as shown in figure 32 and 33 indicates that the buoyancy force raises the air tube whereby the bladder deforms to the deflated condition without folding. On the other hand in figure 33 it becomes clear that the mid section is not as flat as the outer sections while

the air tube is raised enough to create a straight line between the outer ends of the toothpaste tube caps as shown figure 32. The equivalent elastic strain analysis shows maximum strain at the contact points of the air tube/drain with the bladder. This implies that there is elongation in the bladder material, which results in that the circumference of bladder is not equal at any point.
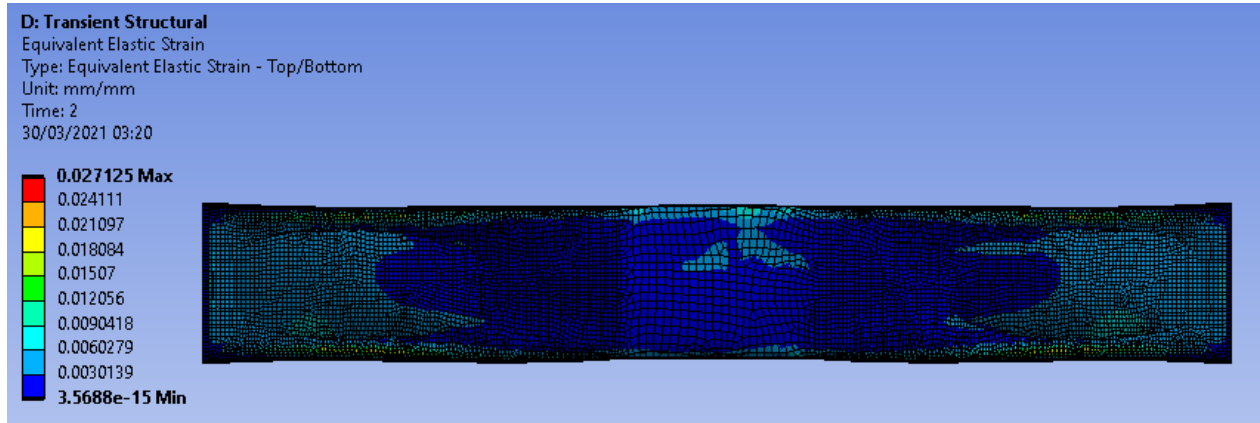


Figure 32: Side view of the preliminary design with toothpaste tube shaped caps at both ends in deflated condition
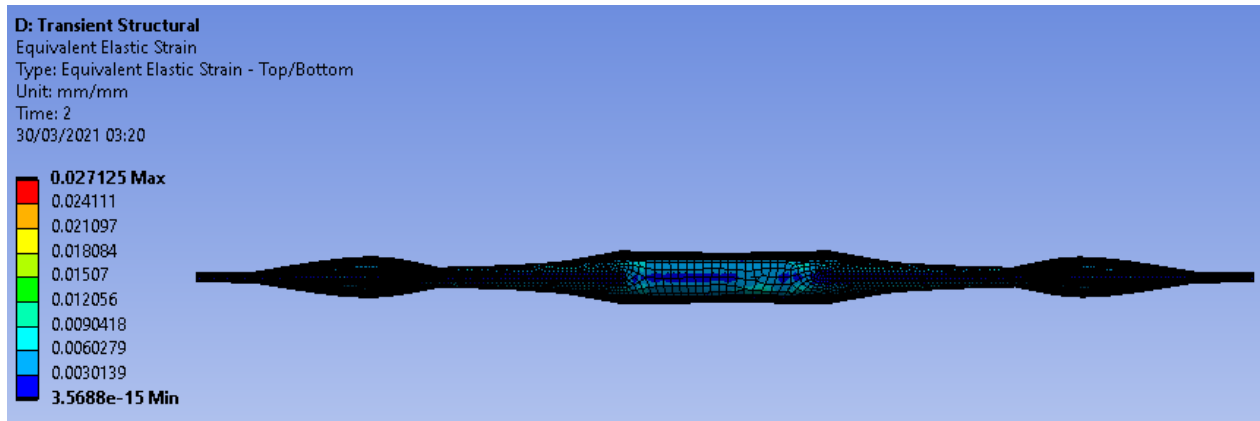


Figure 33: Top view of the preliminary design with toothpaste tube shaped caps at both ends in deflated condition

# 6 Results

This research shows that the principle of the preliminary design has the potential to perform as desired. The drain fixates the bladder at one point while the buoyancy force of the air tube ensures that the material is stretched. In this manner there is no folding of the bladder. A problem that can occur is that side walls make contact during deflation trapping working fluid in the upper compartment.

Furthermore, it becomes clear that round caps do not have the potential to close the ends of the

bladder. The round caps provide to much solidity to the design holding back the deformation at the ends. Due to this aspect a bulge appears on the side of the bladder inducing the bladder to not fully deflate. Furthermore, there is undesirable strain at the contacts points between the bladder and the air tube/drain.

Additionally, a design with pumpkin shaped end caps was created to determine the effect of folding lines. In comparison with the round caps there is clearly a difference. The folding lines take away some of the firmness of the round caps whereby the deflation process performs more effectively. There is no bulge on the side of the bladder and the end caps transform to a more oval shape. However, although there is better performance, the pumpkin shape does not have the potential to be the solution for the preliminary design. The caps still provide to much structure to allow full deflation and result in the same strain behaviour at the air tube/drain as the round caps.

Moreover, the toothpaste tube end caps were simulated to indicate whether the theory of minimal folding by providing a shape that is a blend between full inflated condition and full deflated condition has its effect. The simulations of the cross section of the bladder show that the principle works, the round shape deforms towards the shape of the solid ends without folding. However, the simulation also shows that there is still significant space between the walls at the round end of the bladder; therefore, full deflation is not achieved. Moreover, the equivalent elastic strain analysis indicates strain near the air tube/drain, both objectives which is not desirable either since cyclic strain can eventually lead to failures.

The simulation of the full bladder does show that the principle works with respect to folding; however the midsection of the bladder is not as flat as the end sections which is in alignment with the simulation of the cross section. Furthermore the same level of strain occurs at the contact points with the air tube/drain which also indicates that there is undesired elongation of the bladder material.

# 7    Discussion

All simulations are based on scaled versions of the actual full size designs in order to enable the simulations based on available virtual memory and to shorten the computational times. Although everything is scaled, it is not inconceivable that not all scaling effects are coped with and that performance changes when full size designs are considered.

Besides, the air tube was simulated as a solid body with a force acting on it pretending to be the buoyancy force. In the actual situation the bar is not one solid since it will consist out of a shell and the volume of air inside. Additionally, in the actual situation the buoyancy force arises from the air willing to float since it is submerged, instead of a force acting on the surface of the tube.

Furthermore, during the simulations the designs are not exposed to the current force. Based on the potential of the design of the toothpaste tube caps, the drag coefficient ($C_d$) has to be determined to simulate the current force properly.

The flow is simulated based on the interaction between the fluid and the bladder structure in order to cope with the pressure difference that occurs within the bladder. However, for a more realistic approach two-way-FSI is preferred in which the flow influences the structure and the structure influences the flow.

Moreover, the implementation phase of the engineering cycle (figure 2) has not been reached due to Covid-19 regulations. To prove the usefulness of the toothpaste tube caps it would be wisely to develop an experimental setup based on the toothpaste tube design to determine whether the same behaviour as in the simulation occurs.

# 8 Recommendations

Based on the findings of this research it is recommended to further investigate the toothpaste tube design for the end caps of the preliminary design of the flexible bladder. The first simulations of this design indicate a performance that approaches the requirements of full deflation and minimal folding, although there is some degree of elongation of the bladder material and little undesired volume in the midsection of the bladder. Furthermore, it is recommended to extend the CFD analysis to the usage of two-way-FSI and to a bladder that is fully submerged in a wave-tank, in order to demonstrate if the same promising behaviour is experienced when aspects such as current and buoyancy force are taken into account more detailed. Finally, the development of an experimental setup is recommended to check whether the behaviour of the bladder in real-life is identical to the behavior in the simulation.

# 9 Conclusion

This research has shown that the preliminary design of the OG battery consisting out of a bladder, a drain and an air tube works with respect to deflation and minimal folding. Furthermore, there can be concluded that spherical shapes for closing the ends of the preliminary design have no potential. Even though folding lines are implemented, the spherical shapes apply to much firmness to the design, which lead to poor performance taking into consideration full deflation and strain rates. Next, the toothpaste tube design was tested on full deflation and folding. The design is based on a blend between the circular design of the preliminary design in inflated condition and the oblong design of the preliminary design in deflated condition while maintaining the circumference of the bladder. Based on cross sectional and full bladder simulation there can be concluded that this principle works with respect to folding. Nevertheless, the remaining volume that occurs in the midsection is a downside that requires further research. Altogether, the toothpaste tube shape cap in combination with the preliminary design shows potential regarding folding and is worthwhile to investigate further.

# References

[1]  NASA. "The effects of climate change". In: *Global climate change, vital signs of the planet* (2021).

[2]  H. Ritchie. "Our world in data based on BP statistical review of world energy". In: *ourworldindata.org* (2020).

[3]  Jacopo Torriti. "Understanding the timing of energy demand through time use data: Time of the day dependence of social practices". In: *Energy Research Social Science* 25 (2017), pp. 37–47. ISSN: 2214-6296.

[4]  Roel J Wieringa. *Design science methodology for information systems and software engineering.* Springer, 2014.

[5]  F Ackermann and C Eden. "Strategic Management of Stakeholders: Theory and Practice". In: *Long Range Planning* 44.3 (2011), pp. 179 –196. ISSN: 0024-6301.

[6]  Shirley Gregor and Alan R Hevner. "Positioning and presenting design science research for maximum impact". In: *MIS quarterly* (2013), pp. 337–355.

[7]  Sietse Van den Elzen. "Designing a underwater flexible reservoir". MA thesis. RUG, 2018.

[8]  J.A. Koning. "Studying, designing, creating and testing the bladder reservoir of the Ocean Grazer 3.0". MA thesis. RUG, 2018.

[9]  C.B. Van den Hoek. "Validating the bladder storage system proof-of-concept of Ocean Grazer 3.0 using principles of photogrammetry". MA thesis. RUG, 2019.

[10]  Adityo Kuncorojati. "Fold Structure Detection Analysis during Inflation and Deflation Process on Bladder Reservoir of Ocean Grazer using 3D Finite Element Method". MA thesis. RUG, 2020.

[11]  Andrew J. Pimm, Seamus D. Garvey, and Maxim de Jong. "Design and testing of Energy Bags for underwater compressed air energy storage". In: *Energy* 66 (2014), pp. 496 –508. ISSN: 0360-5442.

[12]  Vegard Lundal and Sigurd van Dijk Festøy. "A Study of a Subsea Chemicals Storage & Injection-Station". MA thesis. NTNU, 2017.

[13]  Anastasia Malea. "Innovative packaging design: toothpaste packaging design case study". In: (2017).

[14]  Laurence W McKeen. *Fatigue and tribological properties of plastics and elastomers.* William Andrew, 2016.

[15]  Qizhou Yao, Jianmin Qu, and G Woodruff. "Three-Dimensional Versus Two-Dimensional Finite Element Modeling of Flip-Chip Packages". In: *To Appear in J. Electronic Packaging* 121 (Sept. 1999). DOI: 10.1115/1.2792684.

[16] Mario Coccia. "The Fishbone diagram to identify, systematize and analyze the sources of general purpose technologies". In: 4 (Dec. 2017), pp. 291–303.

[17] David Wright. *Failure of plastics and rubber products: causes, effects and case studies involving degradation.* iSmithers Rapra Publishing, 2001.

[18] Ib.A. Svendsen and Rene S. Lorenz. "Velocities in combined undertow and longshore currents". In: *Coastal Engineering* 13.1 (1989), pp. 55–79. ISSN: 0378-3839.

[19] Aman I Khalaf, Azza A Ward, and Nehad N Rozik. "Investigation of physical properties and morphology of compatibilized EPDM/EVA blends". In: *Journal of Thermoplastic Composite Materials* 31.3 (2018), pp. 376–391.

[20] DNV DNV-RP. "C205 Environmental conditions and environmental loads". In: *Det Norske Veritas: Oslo, Norway* (2010).

[21] H. Vindenes et al. "Analysis of tidal currents in the North Sea from shipboard acoustic Doppler current profiler data". In: *Continental Shelf Research* 162 (2018), pp. 1 –12. ISSN: 0278-4343.

[22] Ruqiong Qin and Chunyi Duan. "The principle and applications of Bernoulli equation". In: *Journal of Physics: Conference Series* 916 (2017), p. 012038.

[23] Welsim. "The time-domain transient method in structural finite element analysis". In: *Finite Element Analysis Solutions* (2019).

[24] George Lindfield and John Penny. "Chapter 5 - Solution of Differential Equations". In: *Numerical Methods (Fourth Edition).* Ed. by George Lindfield and John Penny. Fourth Edition. Academic Press, 2019, pp. 239–299.

[25] Mikel Ezkurra Mayor et al. "Analysis of One-Way and Two-Way FSI Approaches to Characterise the Flow Regime and the Mechanical Behaviour during Closing Manoeuvring Operation of a Butterfly Valve". In: (2018).

[26] AFAC Masking Systems. *EPDM Material Detail.* 2021. URL: @book{epdmyoung,title={EthylenePropyleneD classrubberdata},author={D2designerdata},year={2021},url={https://afac.co.uk/ materials/epdm/},}.

[27] D2 designer data. *Ethylene Propylene Diene M-class rubber data.* 2021. URL: https:// designerdata.nl/materials/plastics/rubbers/ethylene-propylene-diene-m-class- rubber.

[28] Ronald J Schaefer. "Mechanical properties of rubber". In: *Harris' Shock and Vibration Handbook, Sixth edition, A. Piersol, T. Paez (Eds), McGraw-Hill Companies Inc* (2010), pp. 33– 1.

[29] Russell C Hibbeler. *Statics and mechanics of materials.* Pearson Higher Ed, 2013.

# 10 Appendix

# A EPDM Detail Properties

Rubber Material Selection Guide EPDM or Ethylene Propylene

- Abbreviation                                    EP, EPR, EPT, EPDM
- ASTM D-2000 Classification                      AA, BA, CA, DA
- Chemical Definition                             ethylene propylene diene
- RRP Compound Number Category                    80000 Series

## Physical & Mechanical Properties

- Durometer or Hardness Range          30 – 90 Shore A
- Tensile Strength Range               500 – 2,500 PSI
- Elongation (Range %)                 100 % – 700 %
- Abrasion Resistance                  Good
- Adhesion to Metal                    Good to Excellent
- Adhesion to Rigid Materials          Good to Excellent
- Compression Set                      Poor to Excellent
- Flex Cracking Resistance             Good
- Impact Resistance                    Very Good
- Resilience / Rebound                 Fair to Good
- Tear Resistance                      Fair to Good
- Vibration Dampening                  Fair to Good

## Chemical Resistance

- Acids, Dilute                        Excellent
- Acids, Concentrated                  Excellent
- Acids, Organic (Dilute)              Excellent
- Acids, Organic (Concentrated)        Fair to Good
- Acids, Inorganic                     Excellent
- Alcohol's                            Good to Excellent

## Chemical Resistance

- Aldehydes — Good to Excellent
- Alkalies, Dilute — Excellent
- Alkalies, Concentrated — Excellent
- Amines — Fair to Good
- Animal & Vegetable Oils — Good
- Brake Fluids, Non-Petroleum Based — Good to Excellent
- Diester Oils — Poor
- Esters, Alkyl Phosphate — Excellent
- Esters, Aryl Phosphate — Excellent
- Ethers — Fair
- Fuel, Aliphatic Hydrocarbon — Poor
- Fuel, Aromatic Hydrocarbon — Poor
- Fuel, Extended (Oxygenated) — Poor
- Halogenated Solvents — Poor
- Hydrocarbon, Halogenated — Poor
- Ketones — Good to Excellent
- Lacquer Solvents — Poor
- LP Gases & Fuel Oils — Poor
- Mineral Oils — Poor
- Oil Resistance — Poor
- Petroleum Aromatic — Poor
- Petroleum Non-Aromatic — Poor
- Refrigerant Ammonia — Good
- Refrigerant Halofluorocarbons — R-12, R-13
- Refrigerant Halofluorocarbons w/ Oil — Poor
- Silicone Oil — Excellent
- Solvent Resistance — Poor

## Thermal Properties

- Low Temperature Range     $-60°$ F to $-40°$ F
- Minimum for Continuous Use (Static)     $-60°$ F
- Brittle Point     $-70°$ F
- High Temperature Range     $+220°$ F to $+300°$ F
- Maximum for Continuous Use (Static)     $+300°$ F

## Environmental Performance

- Colorability     Good to Excellent
- Flame Resistance     Poor
- Gas Permeability     Fair to Good
- Odor     Good
- Ozone Resistance     Good to Excellent
- Oxidation Resistance     Excellent
- Radiation Resistance     Good to Excellent
- Steam Resistance     Excellent
- Sunlight Resistance     Excellent
- Taste Retention     Good to Excellent
- Weather Resistance     Excellent
- Water Resistance     Excellent